Three-Dimensional Airflow Through Fronts and Midlatitude Cyclones

Importance of Air Flows

- Great insights into cyclone structures and evolution can be derived from understanding the air flows in midlatitude systems.
- Great advances have been possible during the past several decades using model output.
- Air flows and trajectories provide a more fundamental understanding than traditional (frontal) approaches. (Not all key structures are associated with fronts!)

Some History

1800's

- Thermal Theory conceptual model was dominant in the 1830s and for several subsequent decades.
- Warm core with hurricane-like circulation

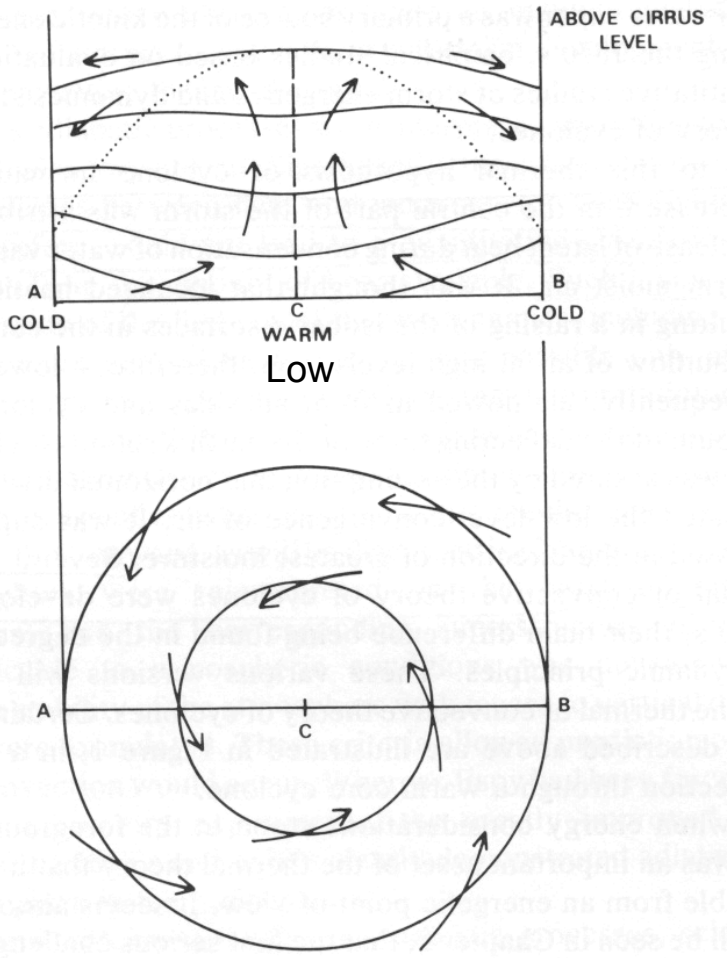

Espy 1831

Major Debates on Cyclone Airflows During the Mid-1800s

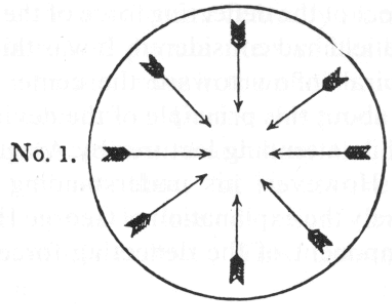

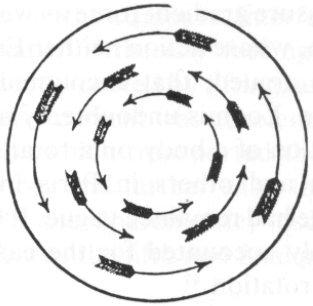

Espy

Redfield

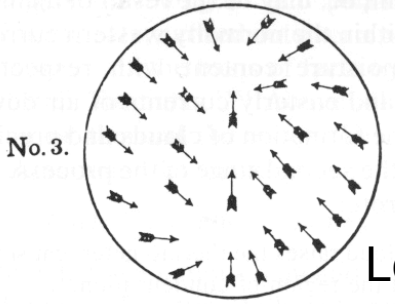

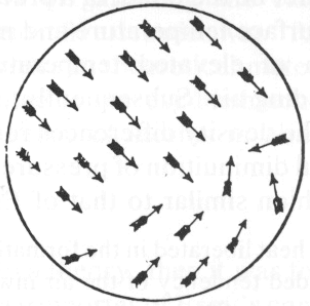

Loomis

FIGURE 9. Diagrams of surface winds in cyclones: No. 1, according to Espy; No. 2, according to Redfield; Nos. 3 and 4, according to Loomis' own investigations, from Loomis, "On two storms which were experienced throughout the United States in the month of February, 1842," *Trans. Am. Phil. Soc.*, **9** (1846). Loomis' analyses of the wind patterns in two storms clearly indicate the confluence of two different currents and distinct boundaries between these currents.

Loomis (1841): First Air Flow Schematic Over Cold Front

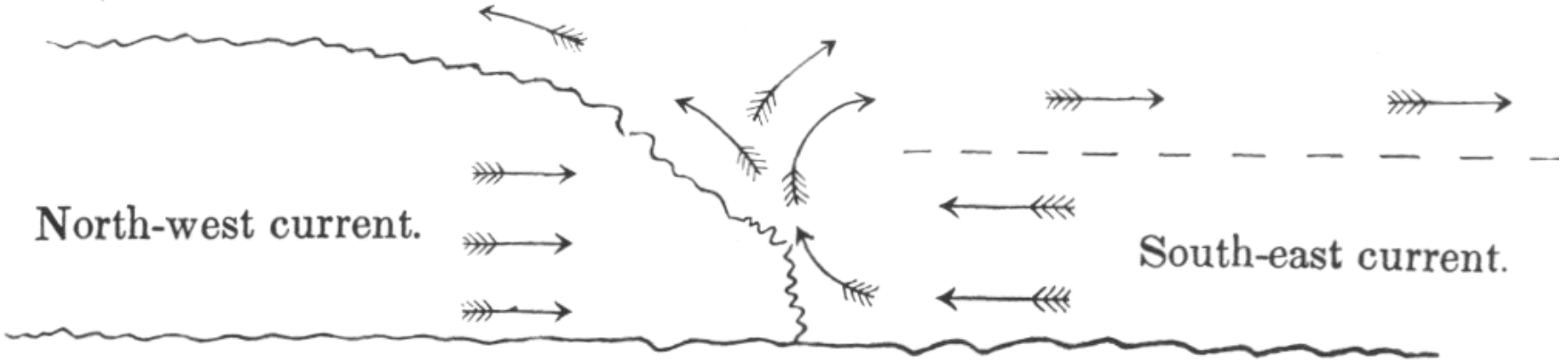

FIGURE 7. Meeting of warm southeast and cold northwest currents of air (Loomis, 1841), from Loomis, "On the storm which was experienced throughout the United States about the 20th of December, 1836," *Trans. Am. Phil. Soc.*, 7 (1841). Loomis' diagram represents the first cross section of what today is called a cold front.

By 1860s the idea of two main airflows (warm and cold) was becoming accepted

Fitz-Roy
1863

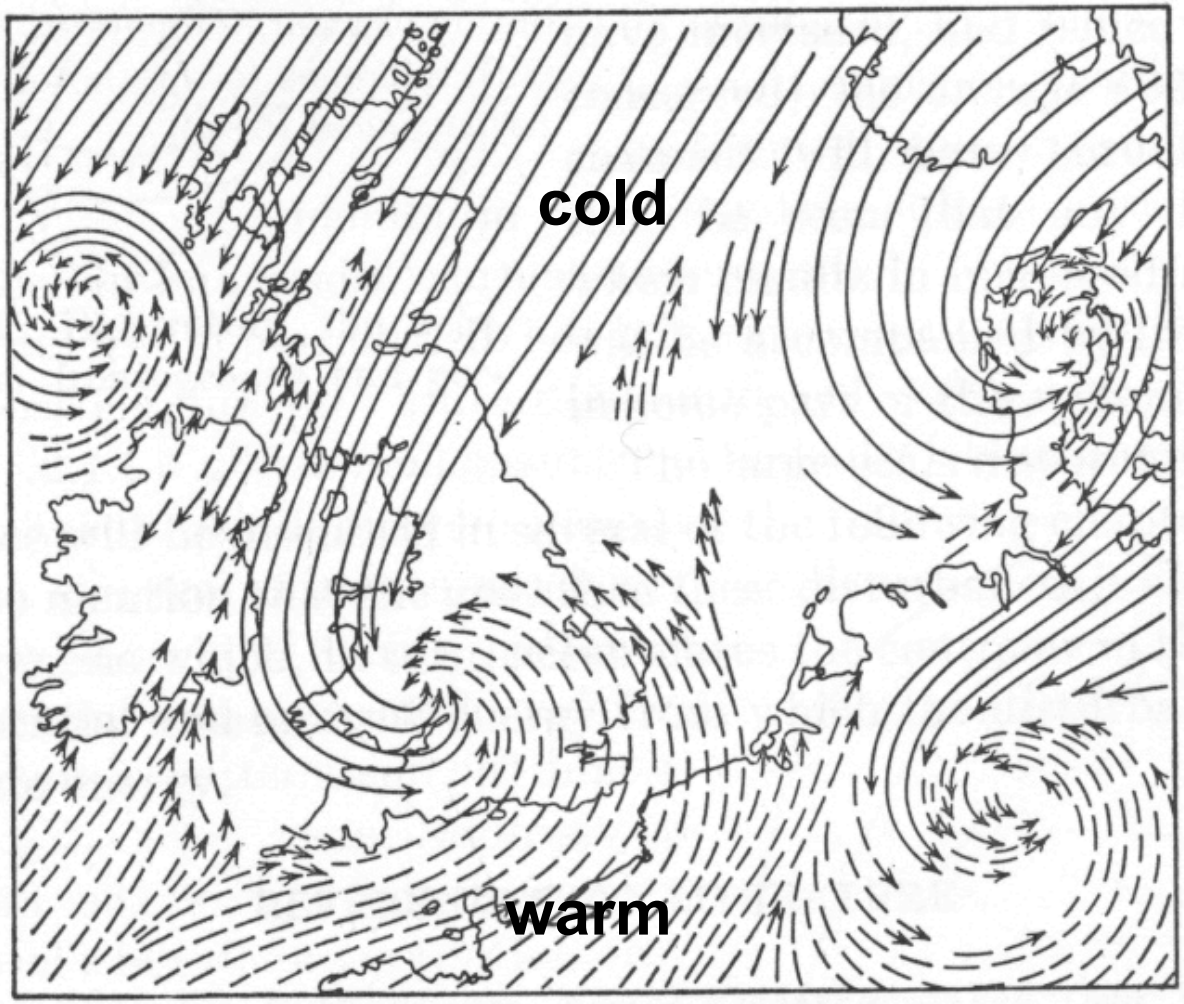

FIG. 12.1.1. Model of extratropical cyclones on the border between tropical and polar air masses. (*After Fitz-Roy*, 1863.)

By the beginning of the 20th century the idea of three main airflows was being suggested.

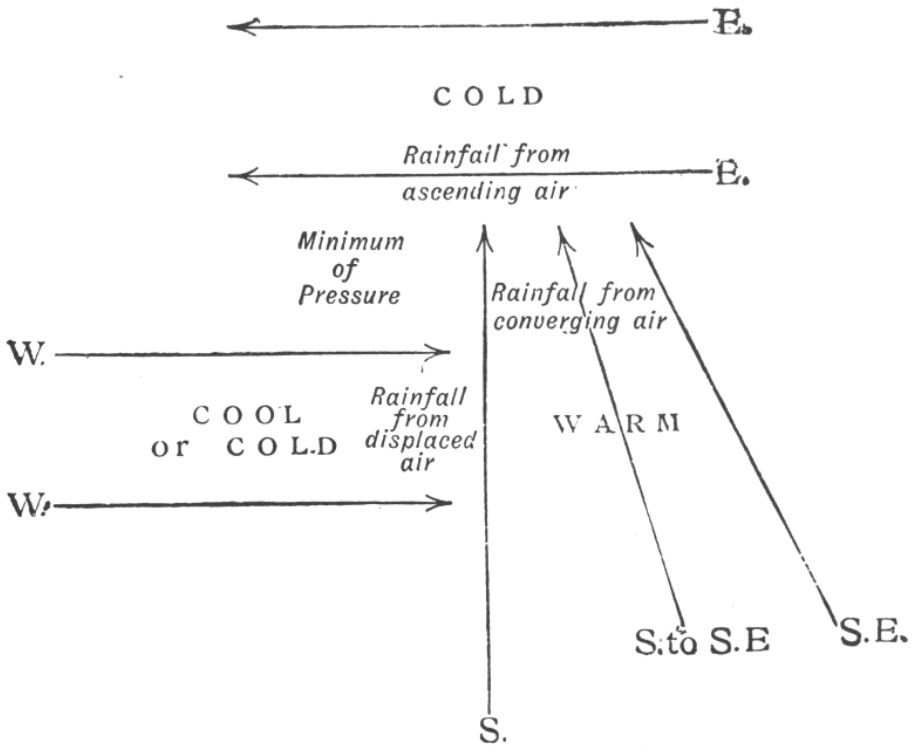

Fig. 19. Shaw's cyclone model (1906/1911). Shaw and R. G. K. Lempfert first published this model in *The Life History of Surface Air-Currents: A Study of the Surface Trajectories of Moving Air* (1906). From Shaw, *Forecasting Weather*, p. 212.

The Norwegian Cyclone Model (Bjerknes 1918 and later) was the First to Connect the Concept of Three-Dimension Airflows with the Clouds and Temperature Structures of Midlatitude Fronts and Cyclones

- A huge advance, but as we will see it had its deficiencies

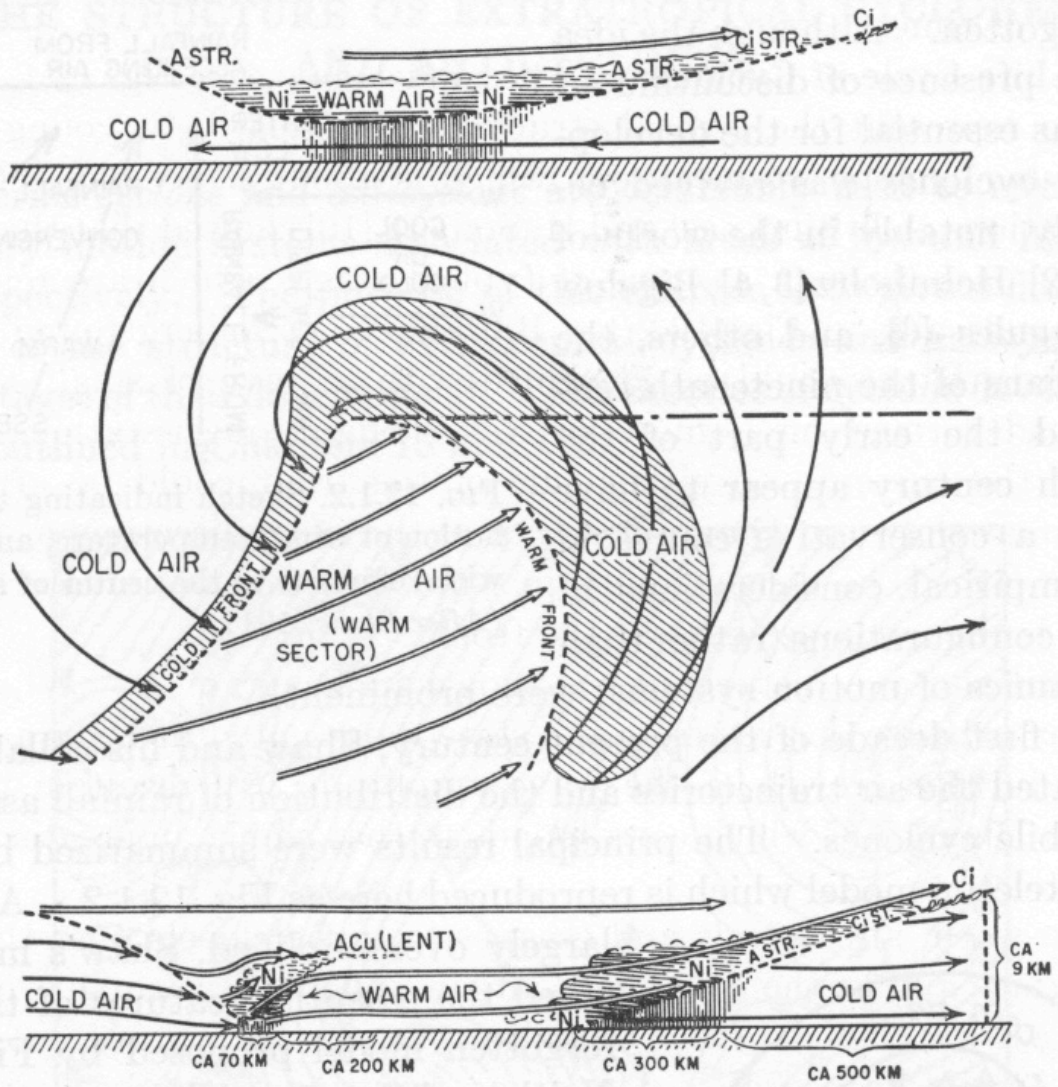

FIG. 12.1.4. Bjerknes' cyclone model. For convenience, this diagram has been reproduced from Bjerknes and Solberg (1921); it contains slight modifications as compared with the original model of J. Bjerknes, 1918.

Norwegian Cyclone Model Concept of Air Flows in Cyclones

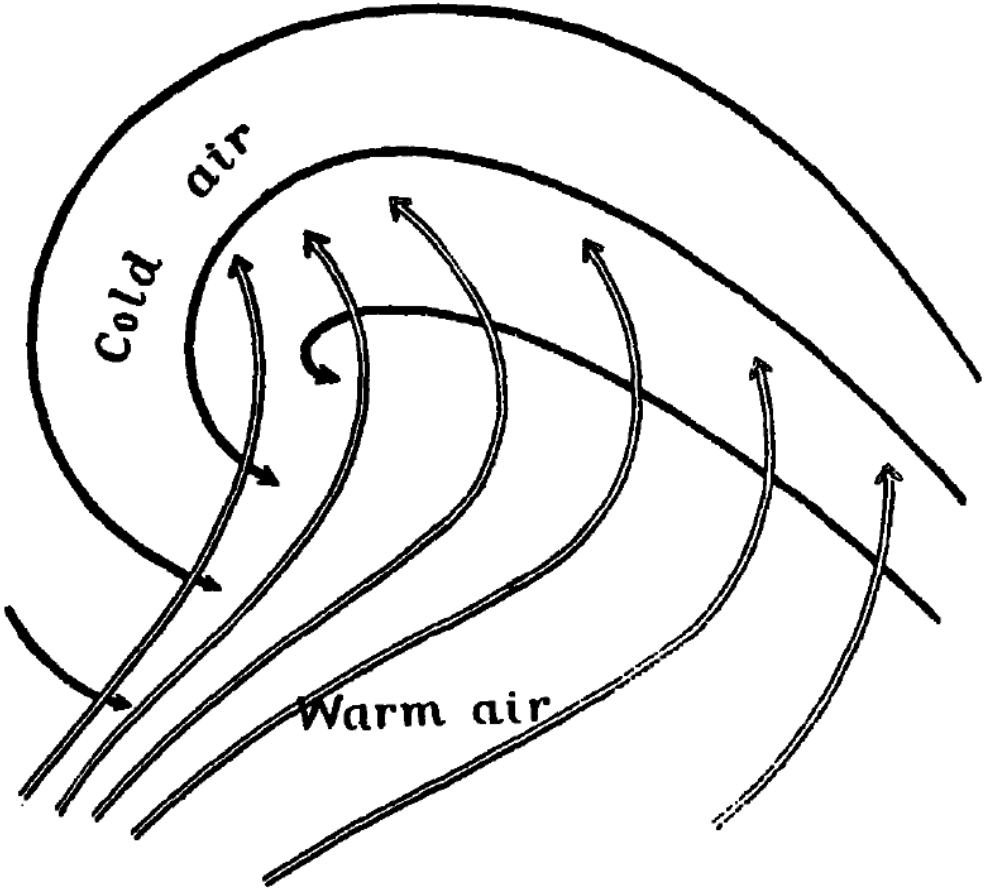

FIG. 6.—Cyclonic motion in lower-air strata.

Missing Key Ingredients

- Dry descending airstreams in the mid to upper troposphere.
- Forward-tilting frontal structures
- Relationships of upper level short wave troughs and ridges with lower tropospheric structures.
- And more…

1930s-1950s

- The availability of radiosonde data painted a revised pictures of three-dimensional airflows and structures.

Palmen and Newton (1969)

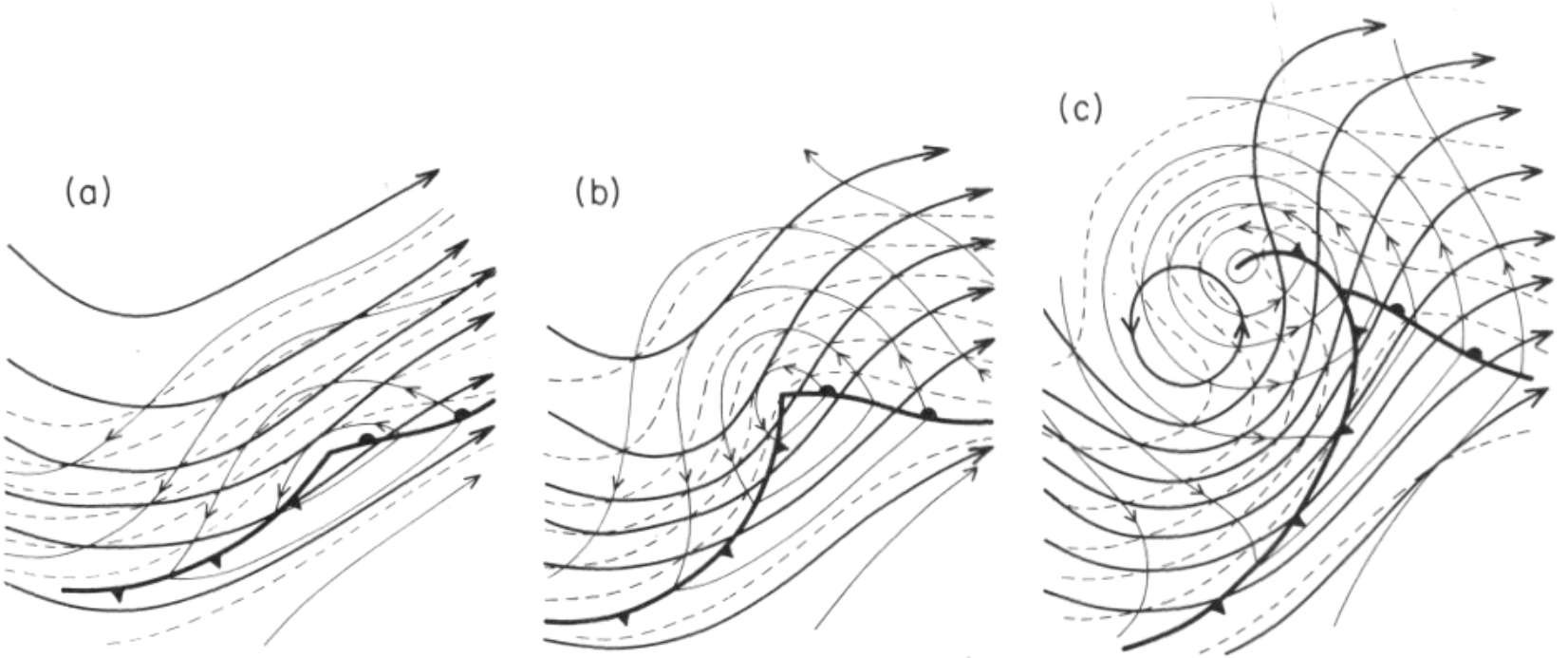

Fig. 3.22 Idealized model of a middle-latitude storm in three stages of development: (a) initial stage, (b) developing stage, and (c) occluded stage. (——) isobars of sea level pressure, (——) contours of 500-mb height, (– – –) contours of 1000–500-mb thickness. (From E. Palmén and C. W. Newton, "Atmospheric Circulation Systems," Academic Press, New York, 1969, p. 326.)

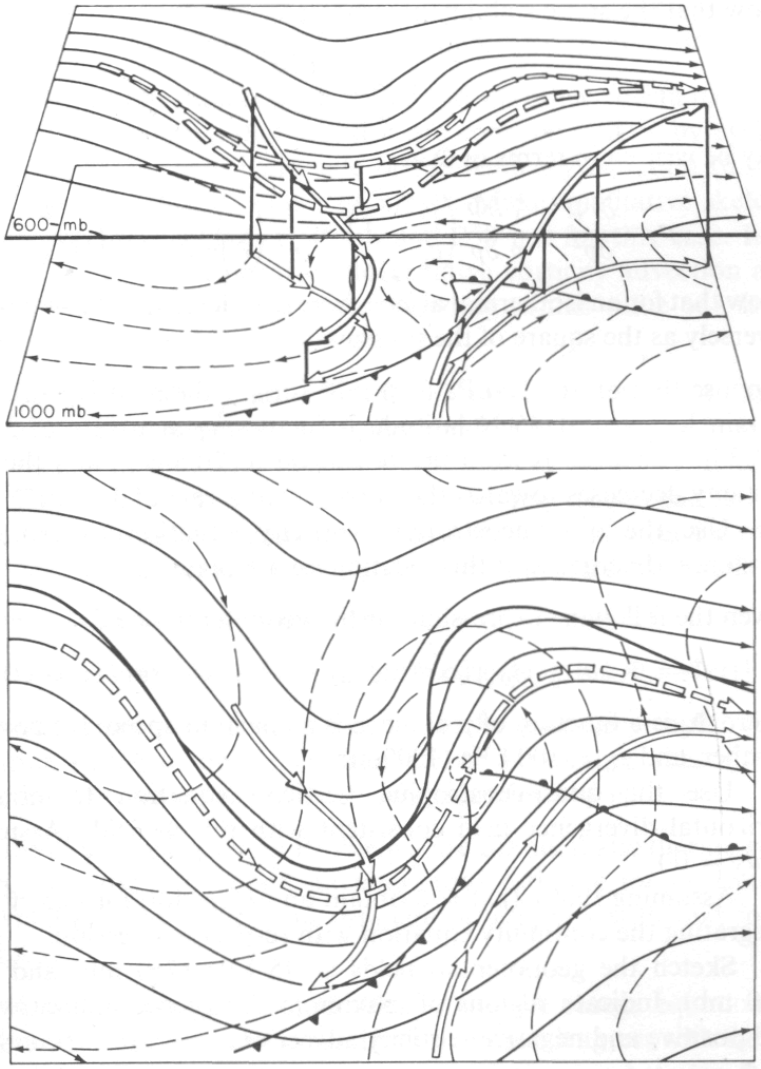

Fig. 6.12 Schematic 600-mb contours (solid) and 1000-mb contours (dashed) for a developing baroclinic wave: upper part gives persepective view indicating selected three-dimensional trajectories (arrows) and their projections on the 1000- or 600-mb surfaces. Dashed trajectory indicates that parcels centered along the 600-mb jet upstream of the developing wave pass through the disturbance approximately along the 600-mb streamlines. However, as shown by the other trajectories, air parcels originating either poleward or equatorward of the jet core are strongly influenced by the vertical motion field associated with the fronts. (After Palmén and Newton,

1950s-1980s

- Many of these studies used relative flow isentropic analysis---assuming system is in steady state and displayed flow relative to the system to give a picture of trajectories and vertical motions.
- Air trajectories follow theta or thetae surfaces depending whether air parcels are unsaturated or saturated.
- Eliassen and Kleinschmidt 57, Browning and Harrold 69, Harold 73, Carlson 80, Browning 86, Young et al., 87, Browning 90

Conveyor Belts

- Many of these studies described the major airflows in cyclones as occurring in a limited number of discrete airstreams or **conveyor belts**.

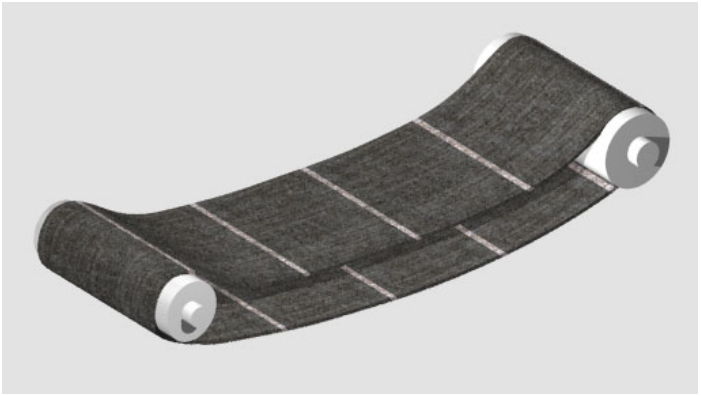

The Conveyor Belt Model of Cyclone Airflows (Carlson, 1980)

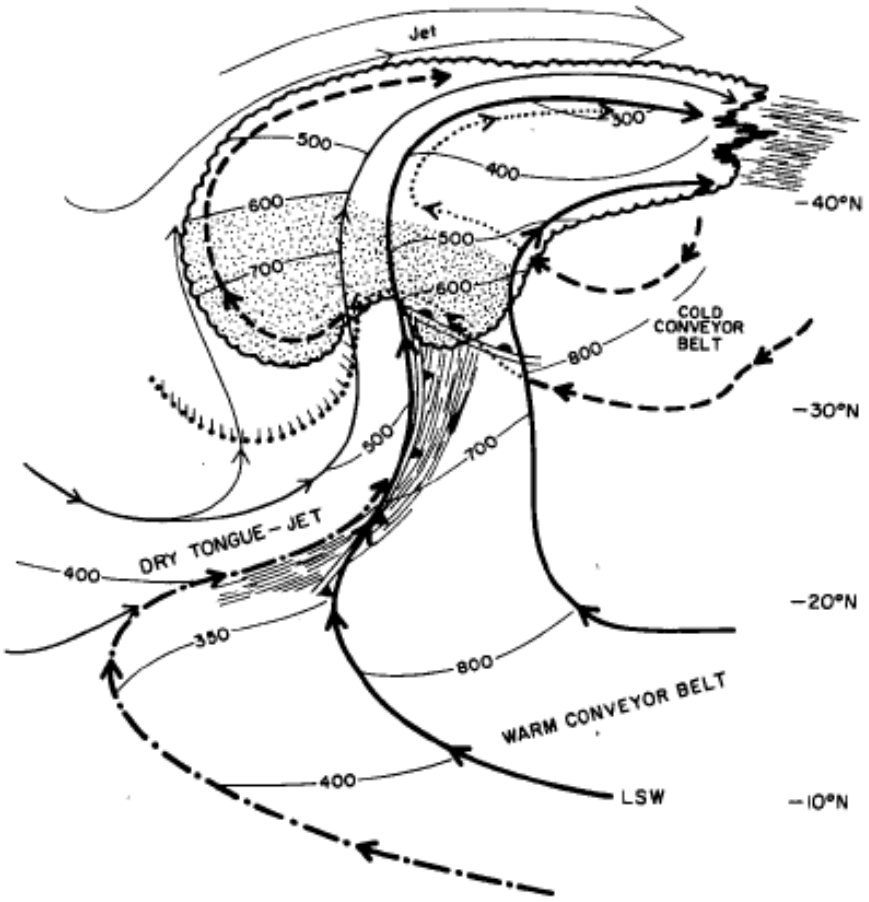

AIRFLOW THROUGH MID-LATITUDE WAVE CYCLONE

FIG. 9. Schematic composite of airflow through middle-latitude cyclone. Heavy solid streamlines depict airflow at top of the warm conveyor belt. Dashed flow represents cold conveyor belt (drawn dotted when it lies beneath the warm conveyor belt or dry airstream.) Dot-dashed flow represents air originating at middle levels in tropics. Thin solid streamlines pertain to dry air which originates at upper levels west of the trough. Thin solid lines denote the heights of the air-streams (mb) and are approximately normal to the direction of the respective air motion; (isobars are omitted for the cold conveyor belt where it lies beneath warm conveyor belt or beneath the jet stream flow). The region of dense upper- and middle-level layer cloud is represented by scalloping and sustained precipitation by stippling. Streaks denote thin cirrus. The edge of the low-level stratus is shown by the curved border of small dots with tails. The major upper tropospheric jet streams are labeled JET. The limiting streamline for the warm conveyor belt is labeled LSW. See text for further explanation.

Clearer Version!

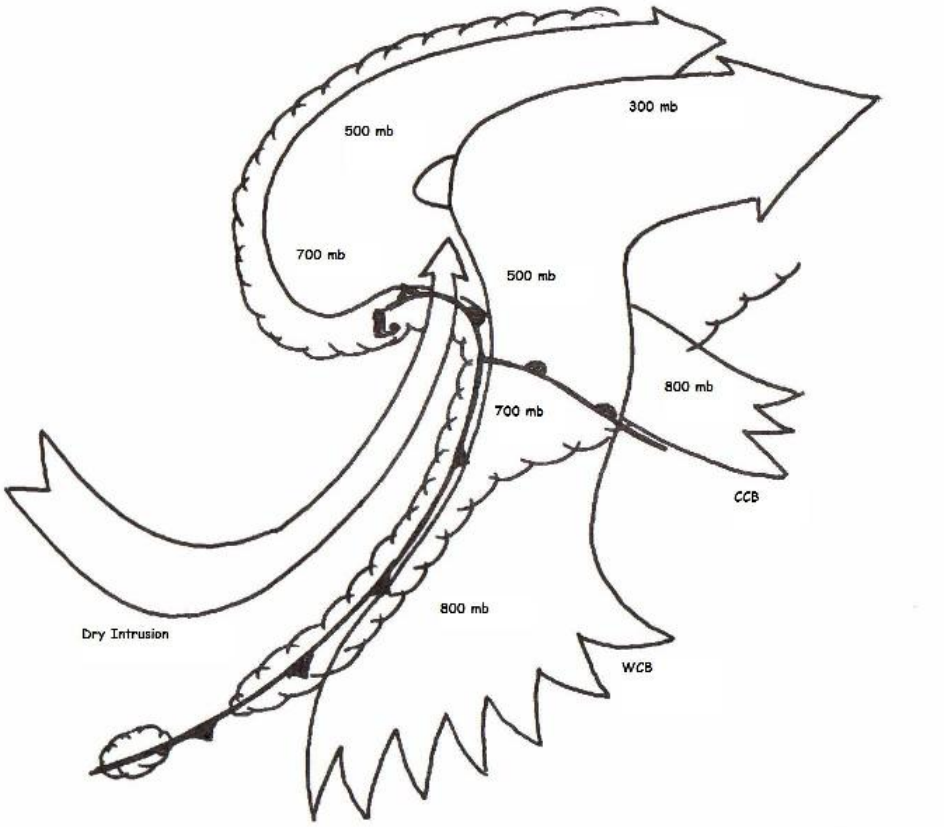

Three Main Airstreams or "Conveyor Belts"

- **Warm conveyor belt** (WCB)
  - associated with most of clouds and precipitation in cyclones.
  - begins at low levels within the southern part of the warm sector and climbs anticyclonically above the warm front.

- **Cold conveyor belt (CCB)**
  - Originates in cold, low-level anticyclonic flow to the northeast of the cyclone and moves westward (relative to the eastward-moving cyclone) north of the warm front.
  - Undercuts the warm conveyor belt (WCB moves over the CCB)
  - Two ideas what happens next:
    - Carlson (1980): Cold conveyor belt then rises and emerges beneath the western edge of the WCB (producing the western extension of the comma head) and then ascends anticyclonically to merge with the WCB.
    - Browning (1990): part of the CCB **descends** cyclonically around the low center to a position behind the cold front.

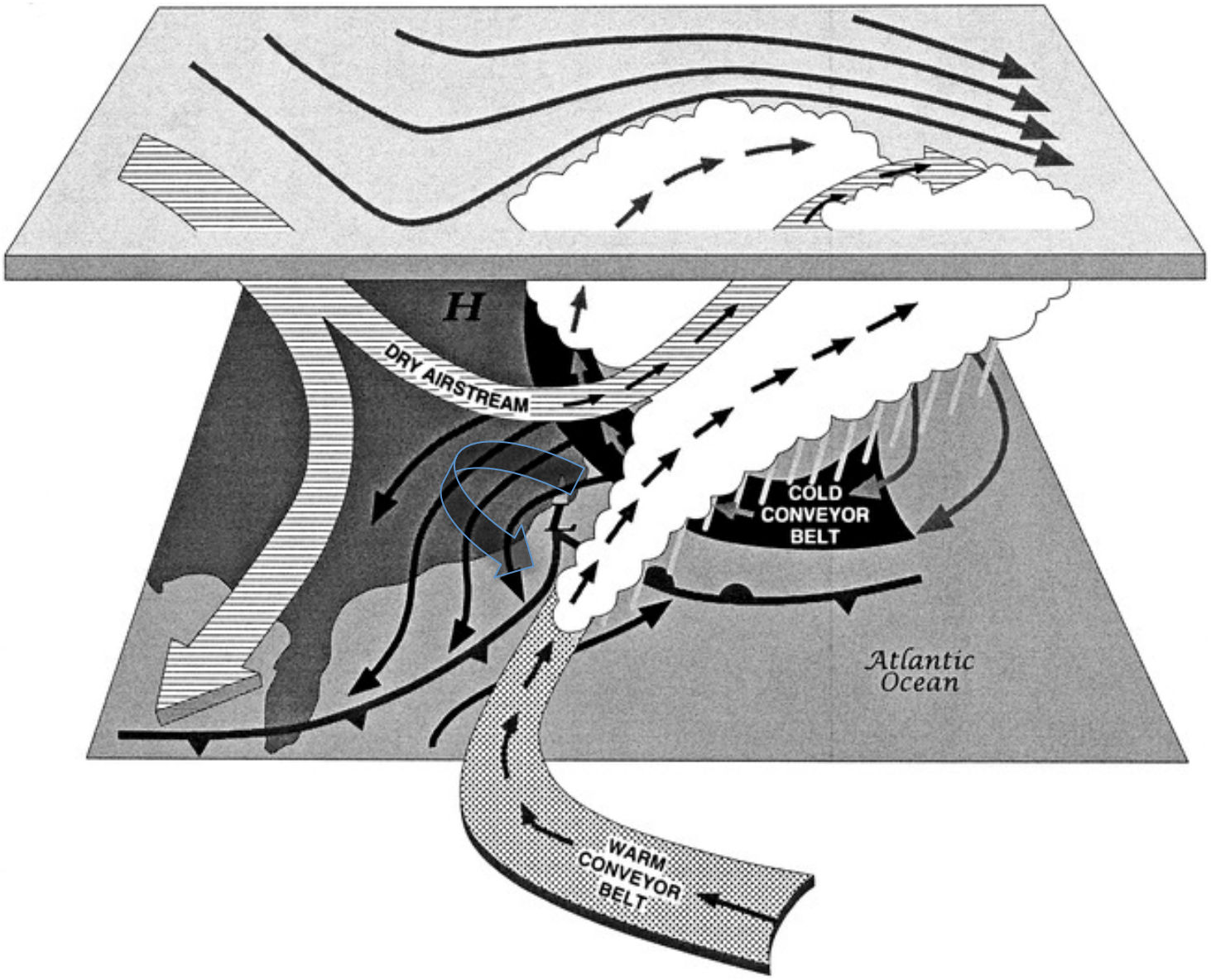
H
DRY AIRSTREAM
COLD
CONVEYOR
BELT
Atlantic
Ocean
WARM
CONVEYOR
BELT

- Dry Airstream or dry intrusion
  - Descends cyclonically from the upper troposphere or lower stratosphere into the lower troposphere and then ascend over the cyclone
  - Often advances over the warm sector of the cyclone
  - The warm sector is often NOT a region of uniform warm, moist air!

Airflow and Conveyor-Belt Studies Have Suggested Structures Not Described in the Norwegian Cyclone Model

Split and Upper "Cold" Front (Browning and Monk 1982)

- Forward-tilting
- Upper front is more of a moisture than temperature front
- Leads to potential instability

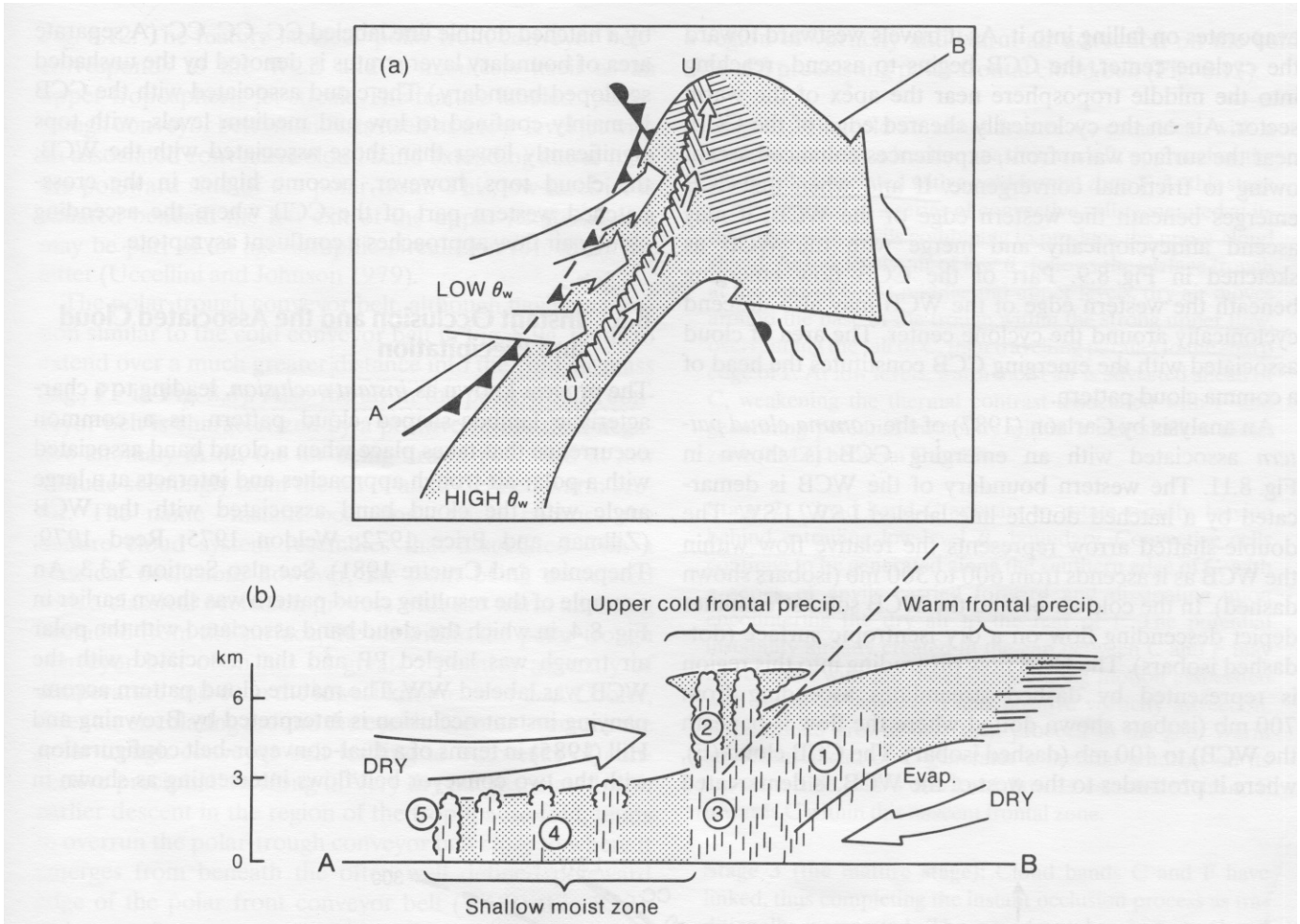

FIG. 8.10. Schematic portrayal of the same situation as in Fig. 8.9, i.e., with the warm conveyor belt undergoing forward-sloping ascent, but drawing attention to the split-front characteristic and the overall distribution of precipitation: (a) plan view; (b) vertical section along AB in (a). In (a) UU represents the upper "cold" front. The hatched shading along UU and ahead of the warm front represents precipitation associated with the upper "cold" front and warm front, respectively. Numbers in (b) represent precipitation type as follows: (1) warm frontal precipitation; (2) convective precipitation-generating cells associated with the upper "cold" front; (3) precipitation from the upper "cold" frontal convection descending through an area of warm advection; (4) shallow moist zone (SMZ) between the upper and surface "cold" fronts, characterized by warm advection and scattered outbreaks of mainly light rain and drizzle; and (5) shallow precipitation at the surface "cold" front itself (Browning and Monk 1982).

Split “Cold” Front

- Often see this on satellite pictures, with a separation between surface front and middle/ upper clouds.

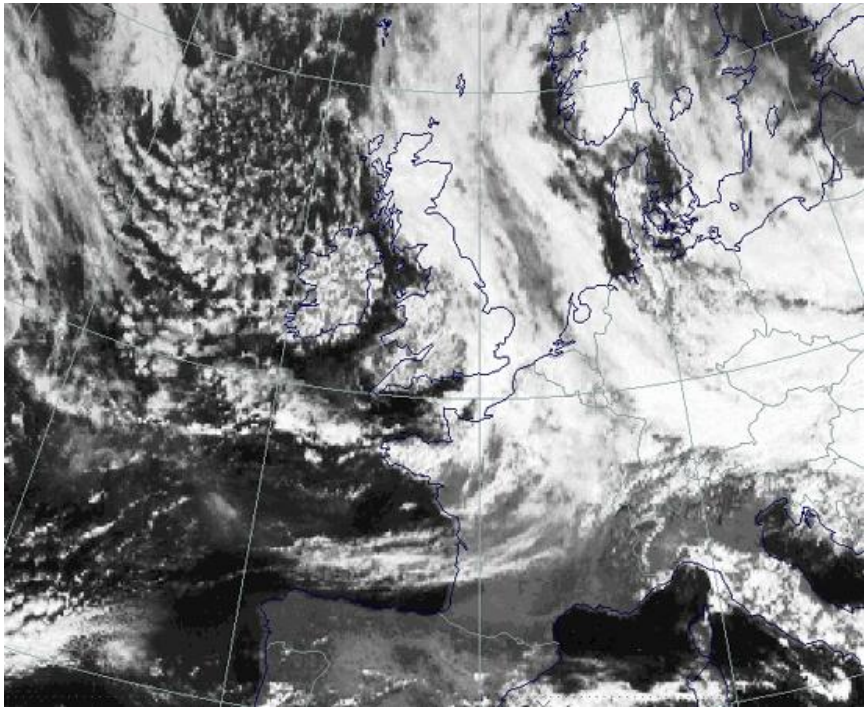

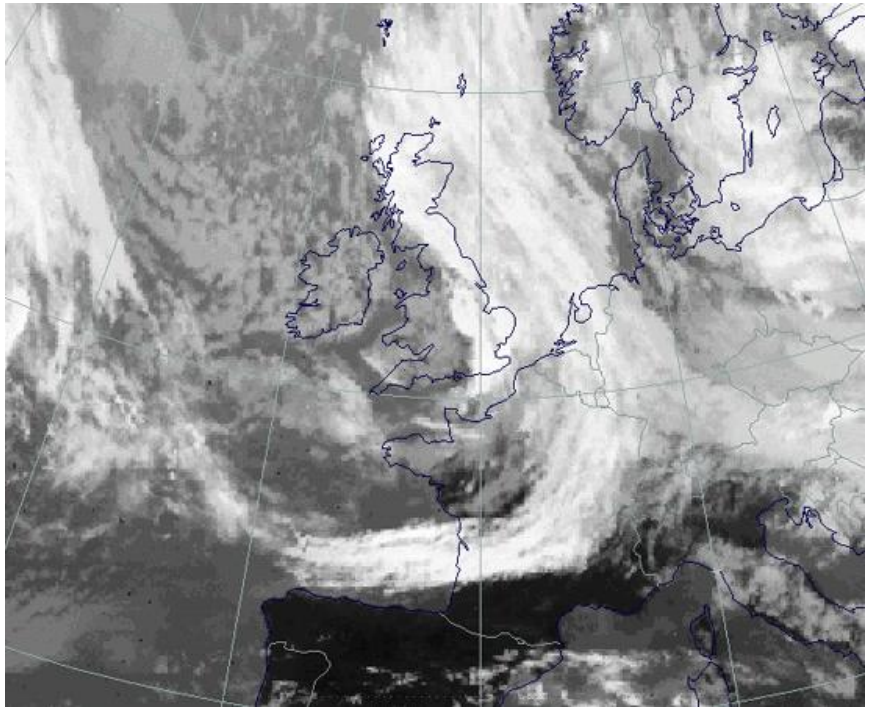

Terminology: Anafront versus Katafront

- **Anafront**: backward leaning. Sinking on cold side and rising motion on warm side.

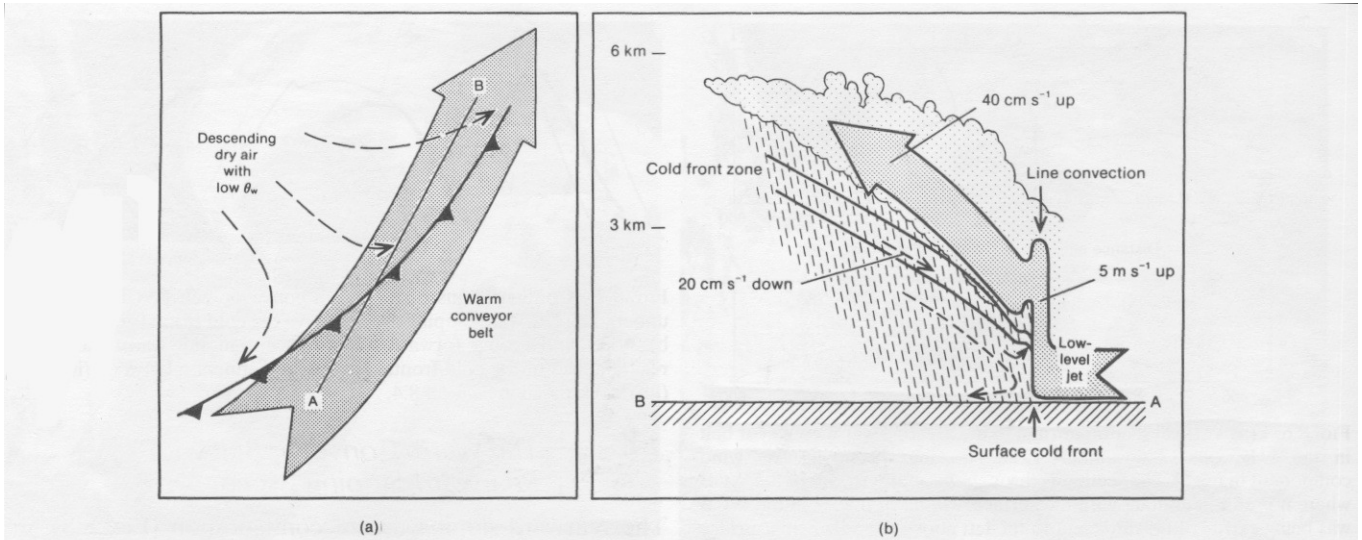

FIG. 8.8. Schematic portrayal of the airflow at a classical ana-cold front showing the warm conveyor belt (bold arrow) undergoing rearward-sloping ascent above the cold frontal zone, with the cold air (dashed lines) descending beneath it: (a) plan view; (b) vertical section along AB in (a). Flows are shown relative to the moving frontal system.

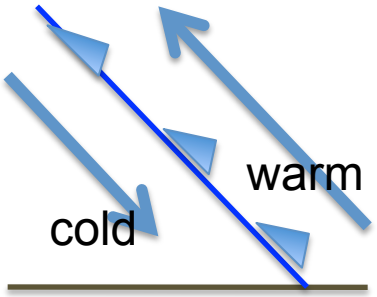

- **Katafront**: descent on both sides of cold front (generally stronger descent on warm side). Not much precipitation with front

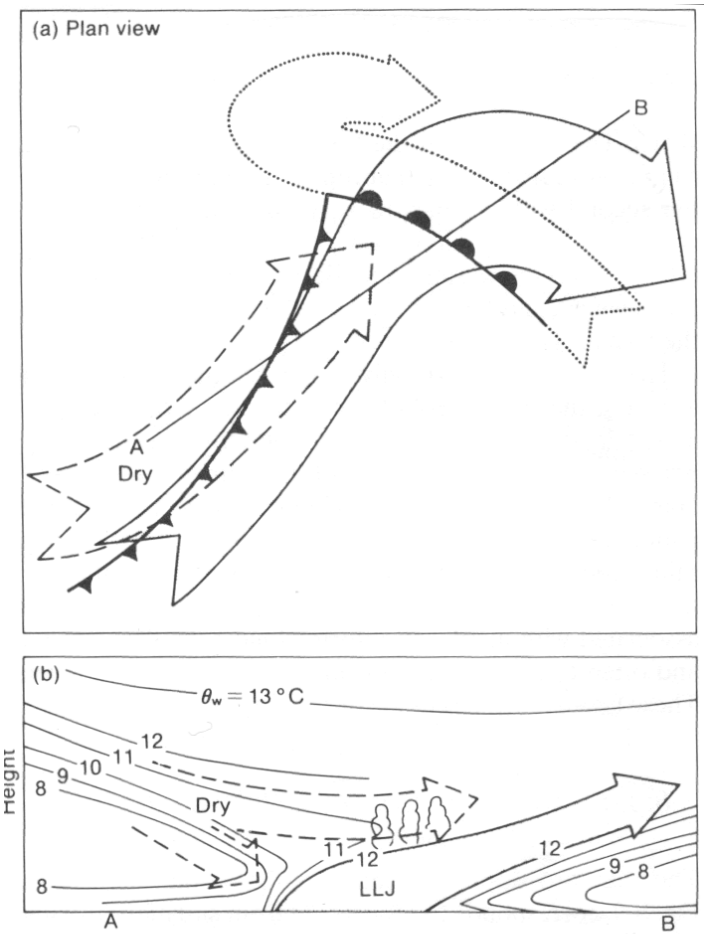

FIG. 8.9. Schematic portrayal of the airflow in an extratropical cyclone in which the warm conveyor belt (solid arrow with stippled shading) is undergoing forward-sloping ascent ahead of a kata-cold front, before rising above a flow of cold air ahead of the warm front (dotted arrow referred to in Section 8.4 as the cold conveyor belt). Middle-tropospheric air with low θ_w (dashed arrow) is shown overrunning the cold front and generating potential instability in the upper portions of the warm conveyor belt. Plan view and vertical section are shown in (a) and (b), respectively, the section in (b) being along the line AB in (a). Flows are shown relative to the moving frontal system.

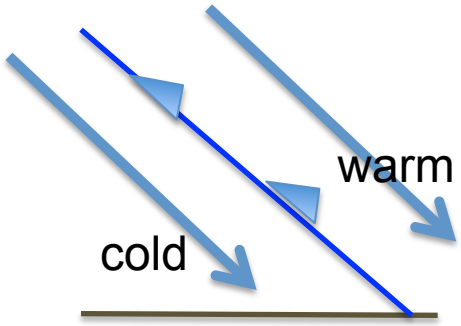

Strengths and Weaknesses of the Conveyor Belt Model

- Strengths
  - If you ignore the details, one can often identify three main broad air streams in cyclones and fronts
  - Gets us away from thinking that all the weather action is related to frontal boundaries. Not only vertical motion is directly related to fronts.
- Weaknessess
  - It is can be a great simplification to consider only three air streams
  - There are all kinds of intermediary trajectories

1980s-now: The Model Revolution

- Realistic model simulation at high resolution allows the creation of three-dimensional trajectories.
- Modern graphics promotes visualization—a major challenge.
- An early example: The President's Day Storm of 1993: http://www.atmos.washington.edu/academic/videos/PresidentsDayStorm.html

Trajectories for a Relatively "Classical" Case over North America: December 14-16, 1987 (Mass and Shultz,1993)

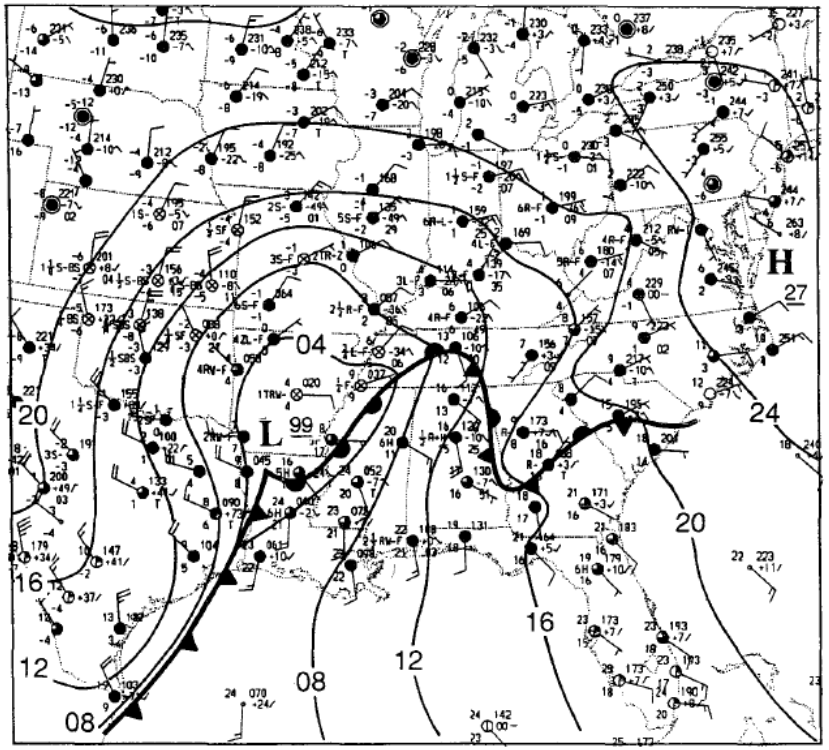

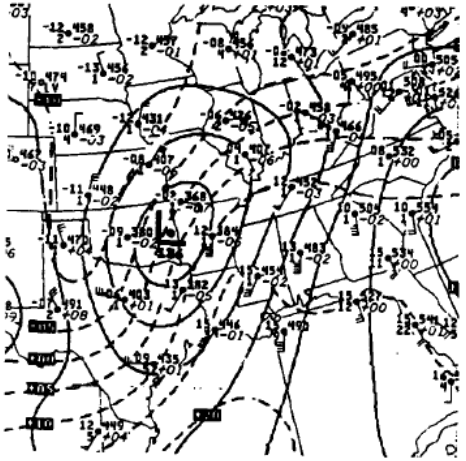

b

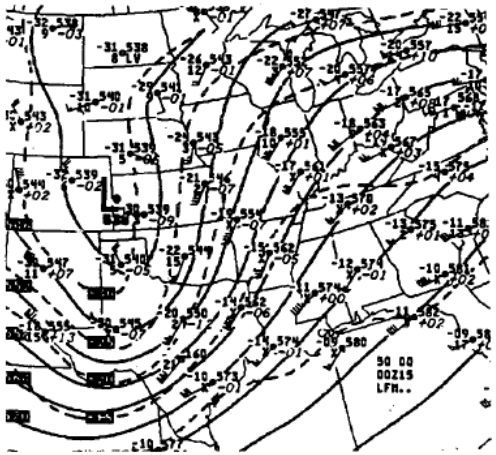

c

FIG. 1. (a) Surface, (b) 850-mb, and (c) 500-mb synoptic analyses at 0000 UTC 15 December 1987.

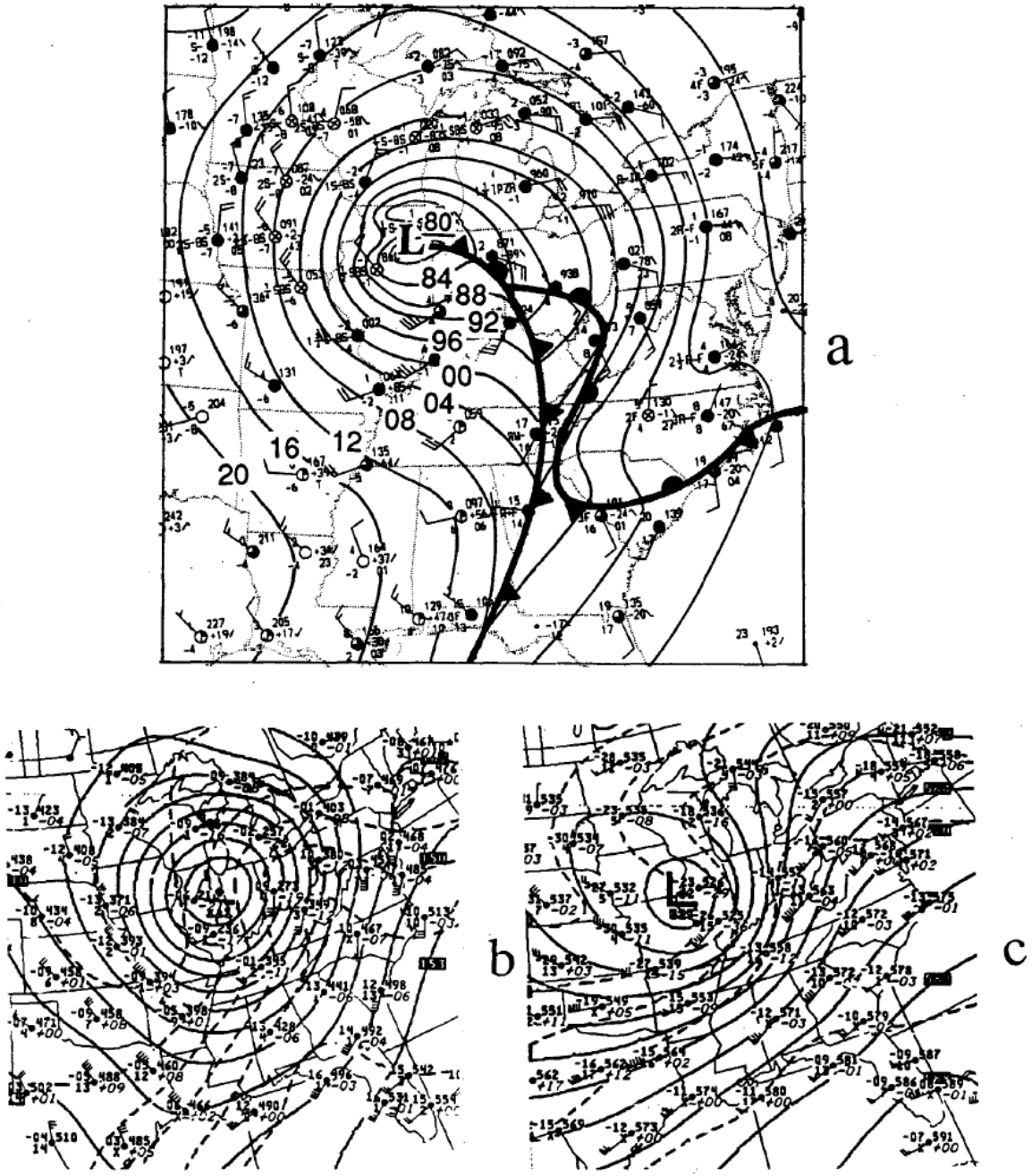

FIG. 2. Same as Fig. 1 but for 1200 UTC 15 December 1987.

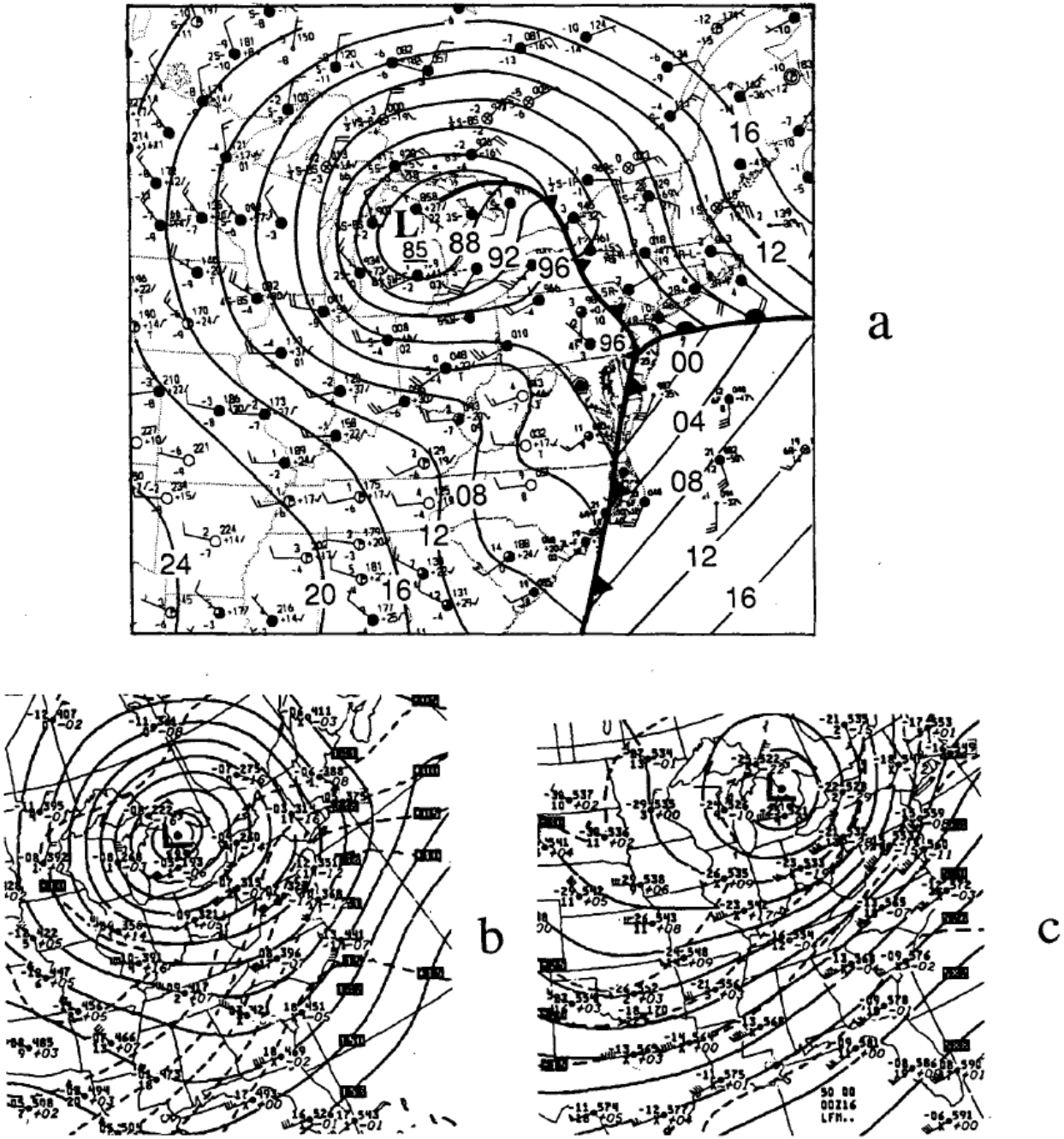

FIG. 3. Same as Fig. 1 but for 0000 UTC 16 December 1987.

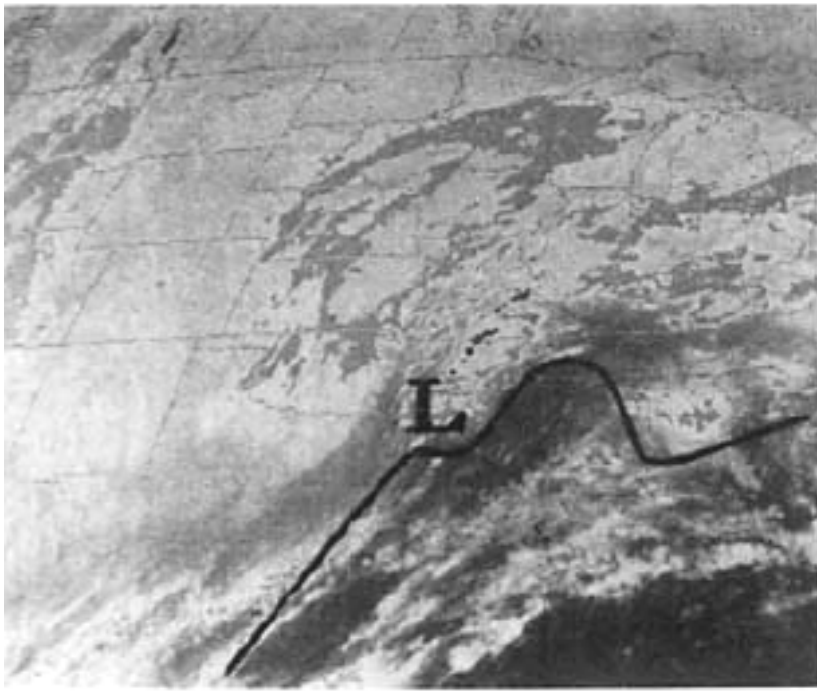

0001 UTC 15 Dec. 1987

1101 UTC 15 Dec. 1987

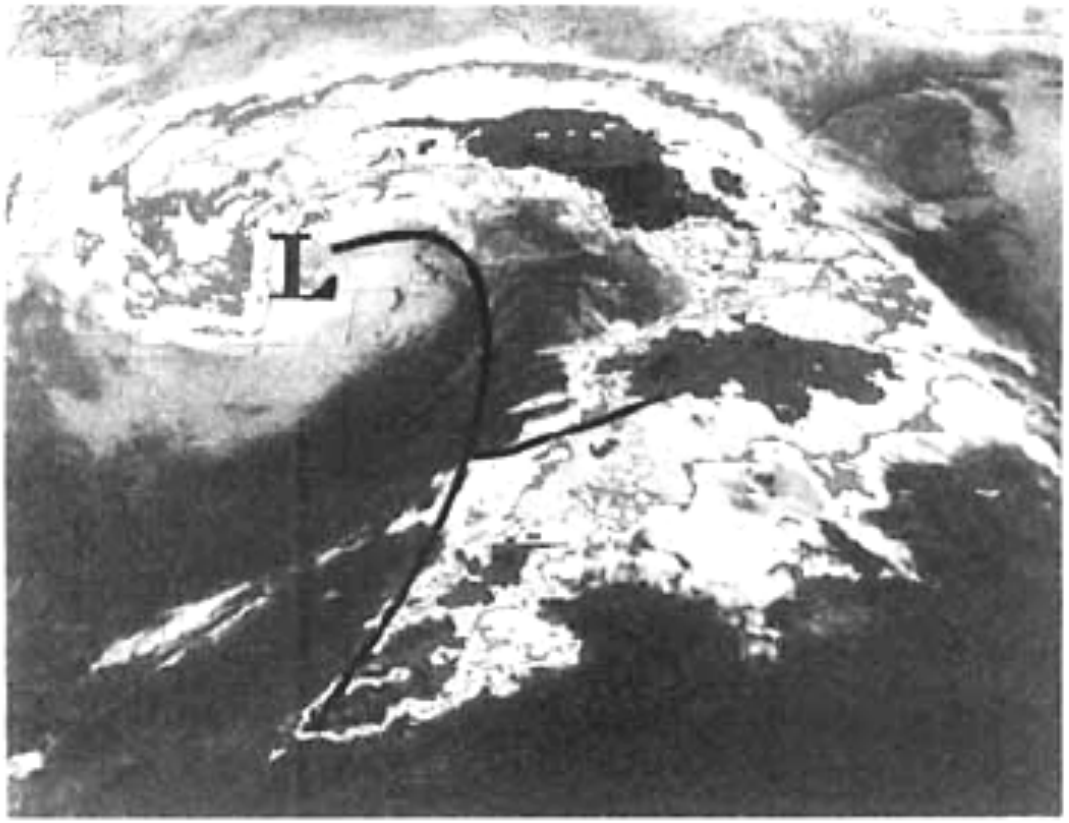

1701 UTC 15 Dec. 1987

0035 UTC 15 December

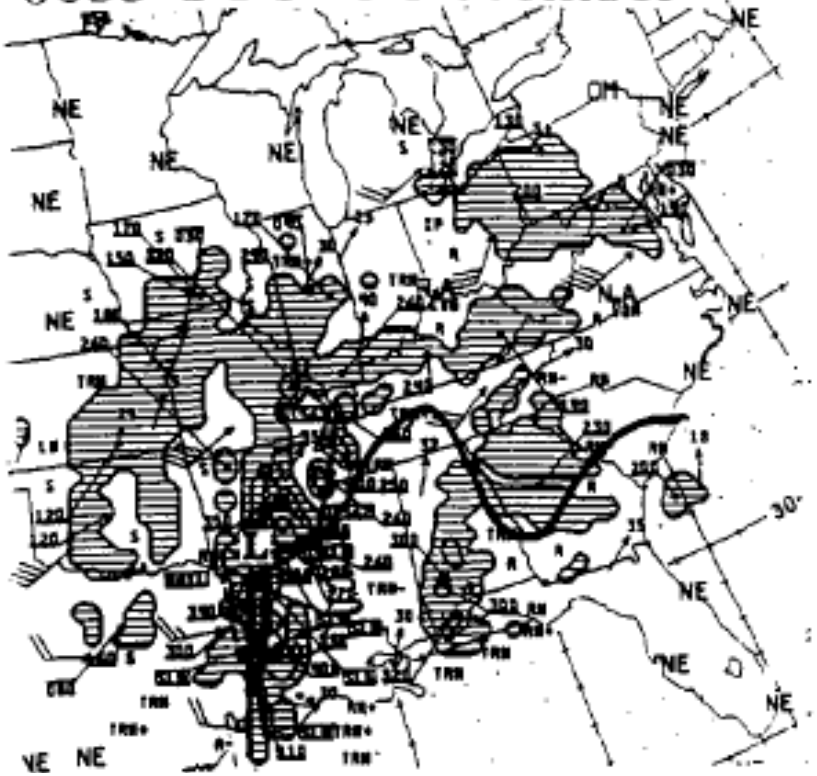

1135 UTC 15 December

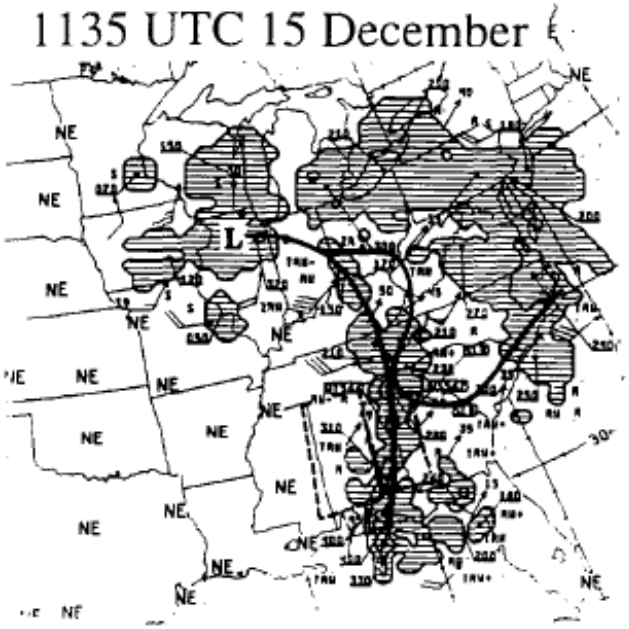

1735 UTC 15 December

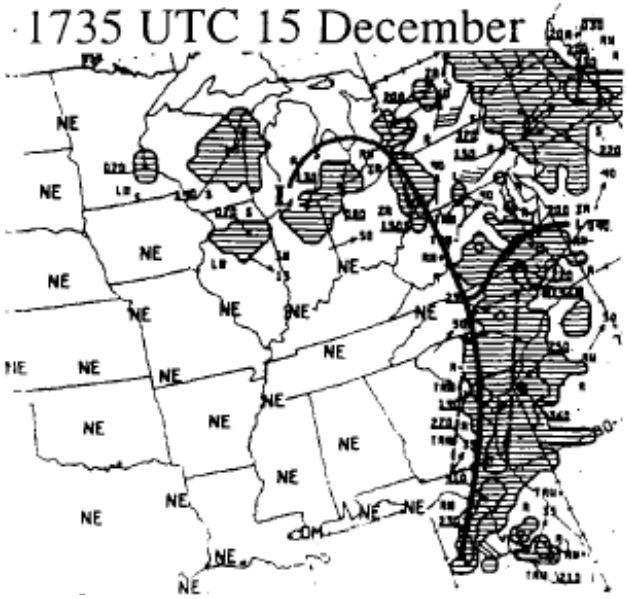

Realistic MM5 Simulation

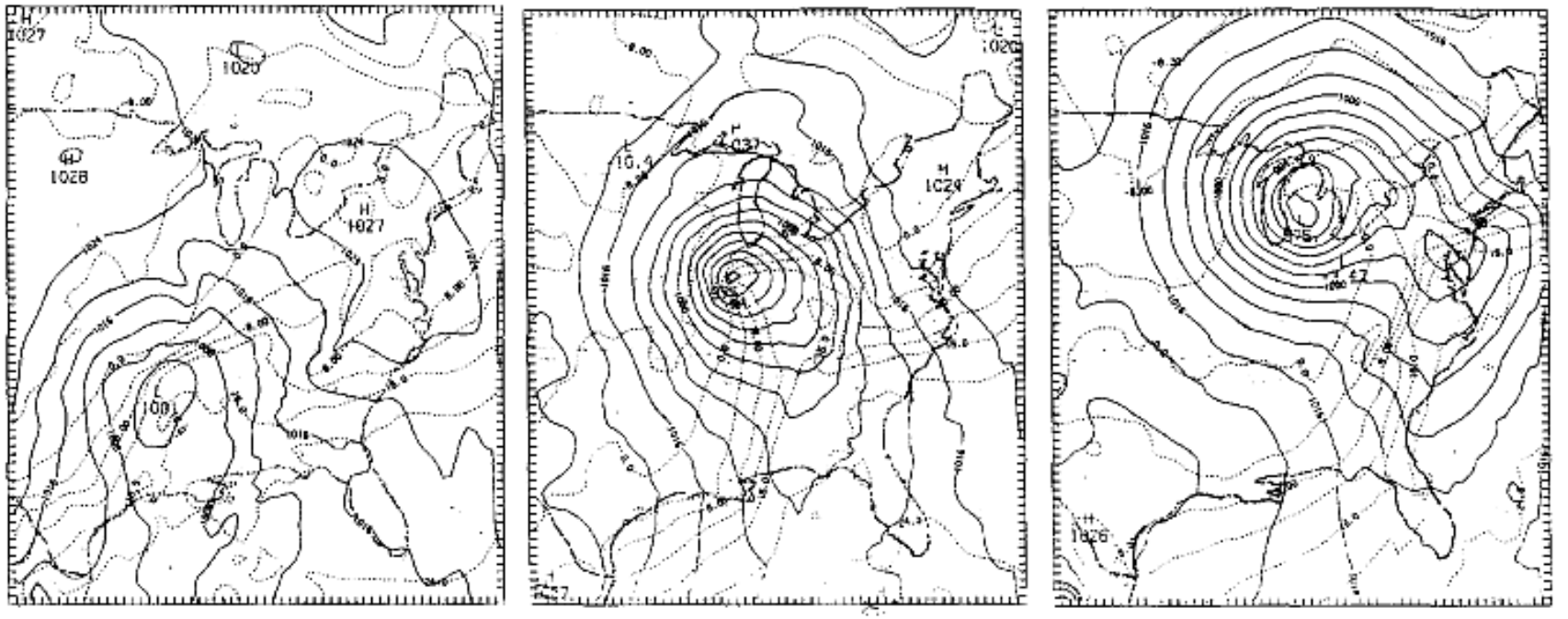

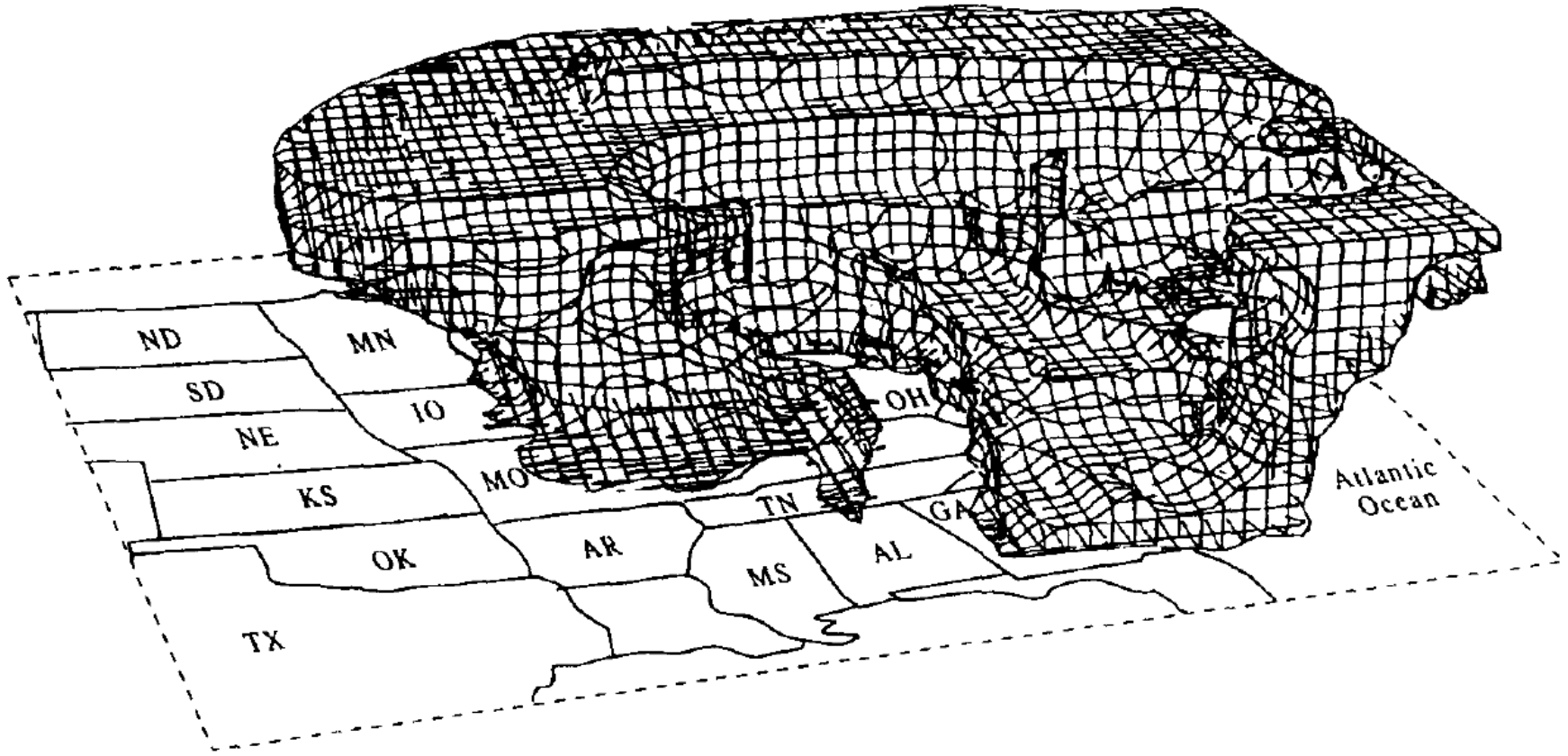

FIG. 10. Three-dimensional perspective from the south of the 100% relative humidity volume of the storm at 30 h into the simulation.

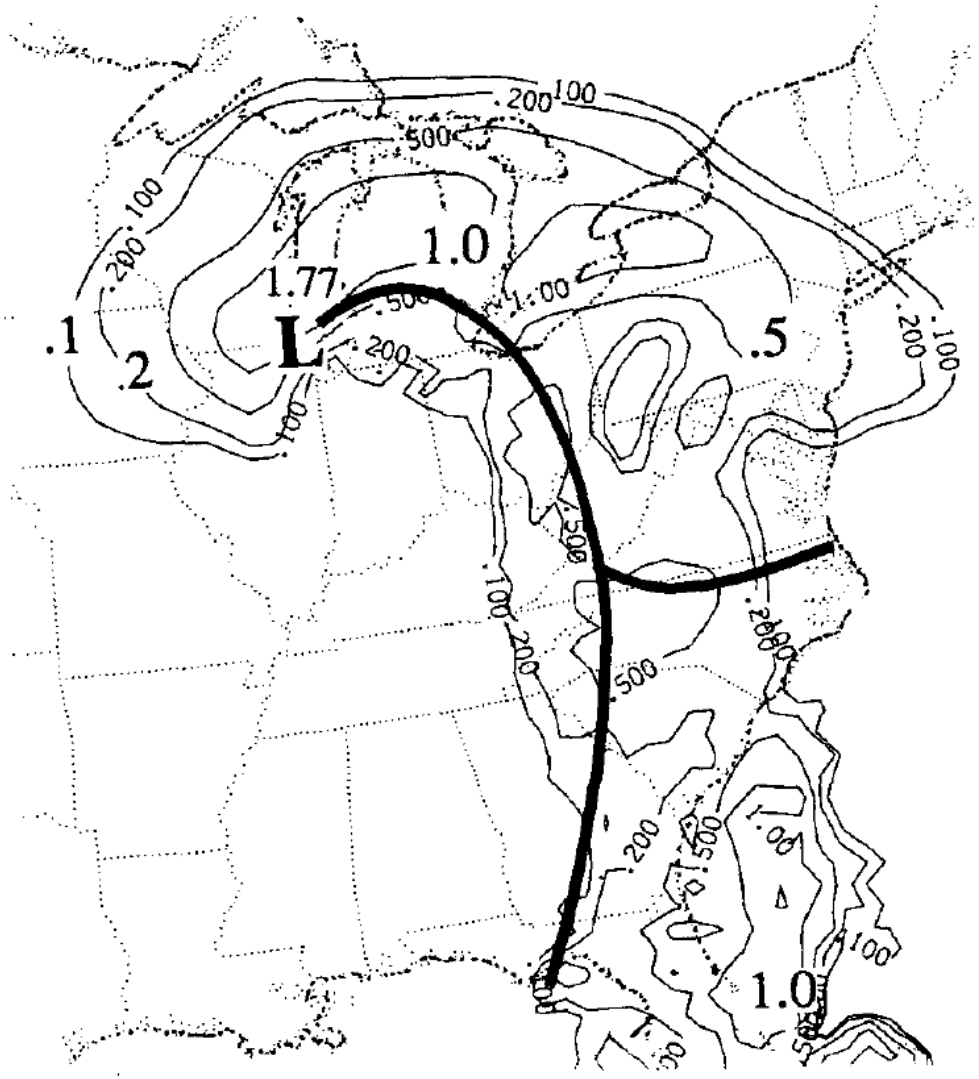

FIG. 11. Total precipitation (cm) for 27–30 h into the simulation (nominally 1500–1800 UTC 15 December 1987). Model surface fronts at 30 h are also shown.

Model-Based Trajectories

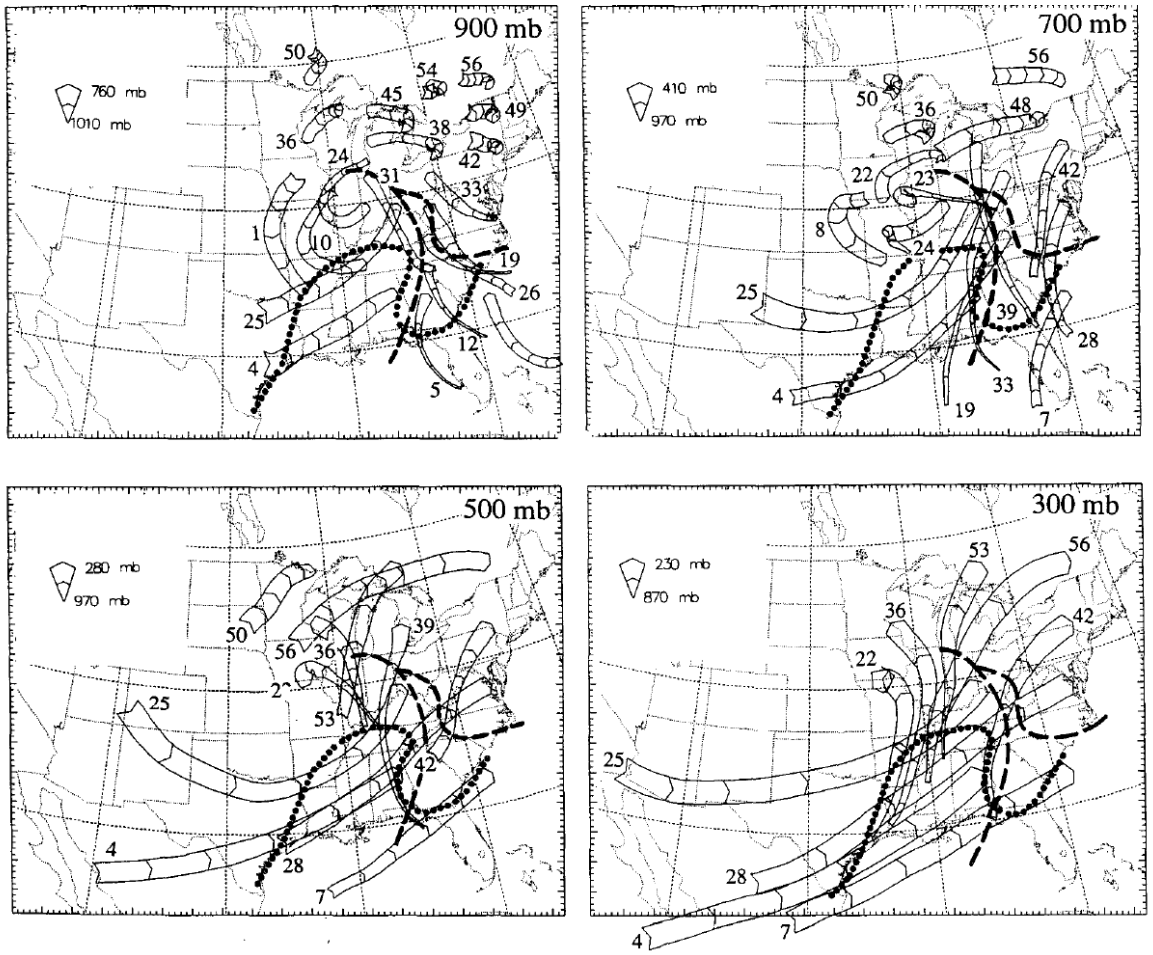

FIG. 18. Backward trajectories taken from 27 to 12 h into the simulation ending at 900, 700, 500, and 300 mb. The model surface frontal positions at 27 h (dashed) and 12 h (dotted) are also shown.

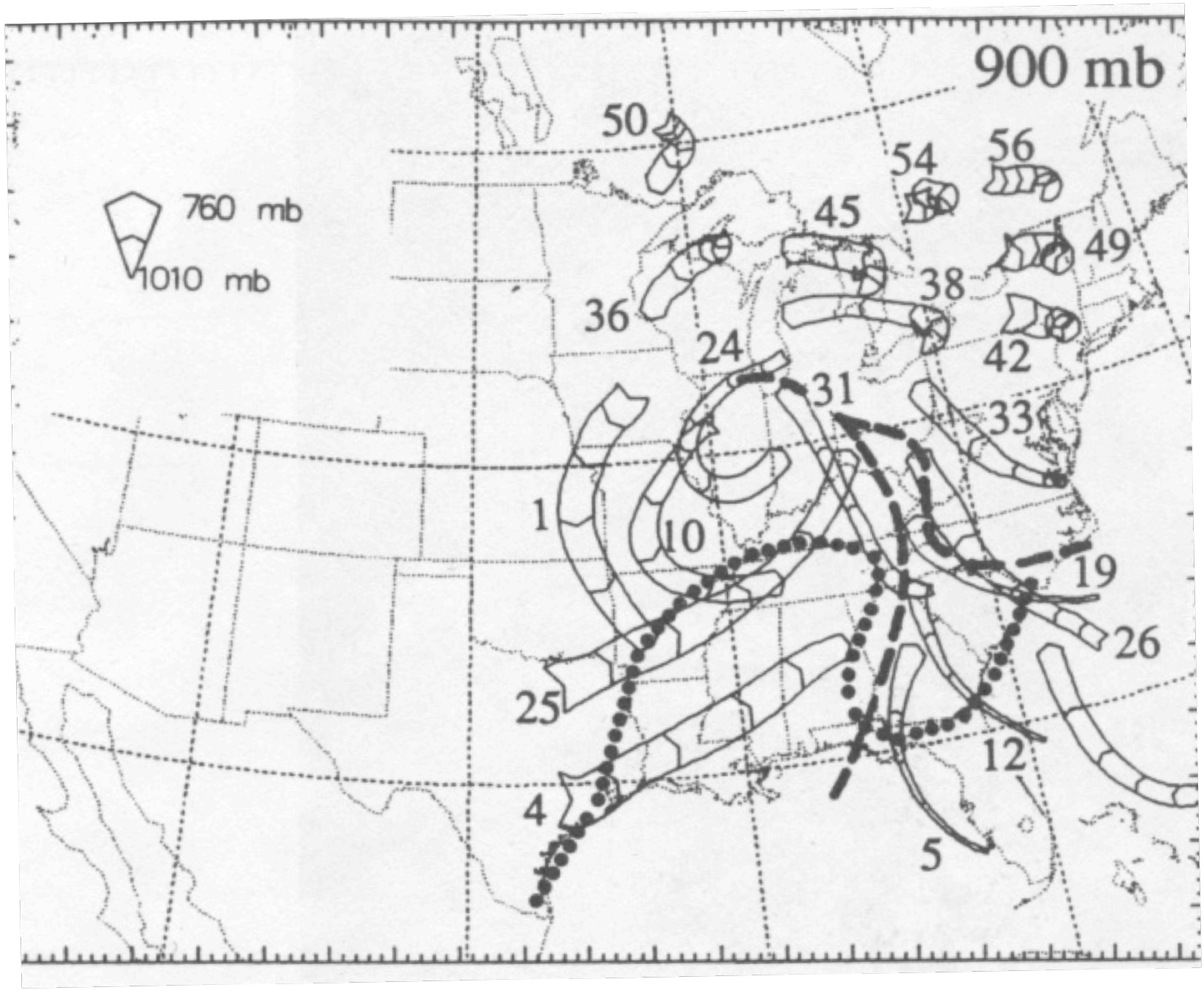
900 mb
760 mb
1010 mb
50
54
56
45
49
38
36
24
42
31
33
1
10
19
26
25
12
4
5

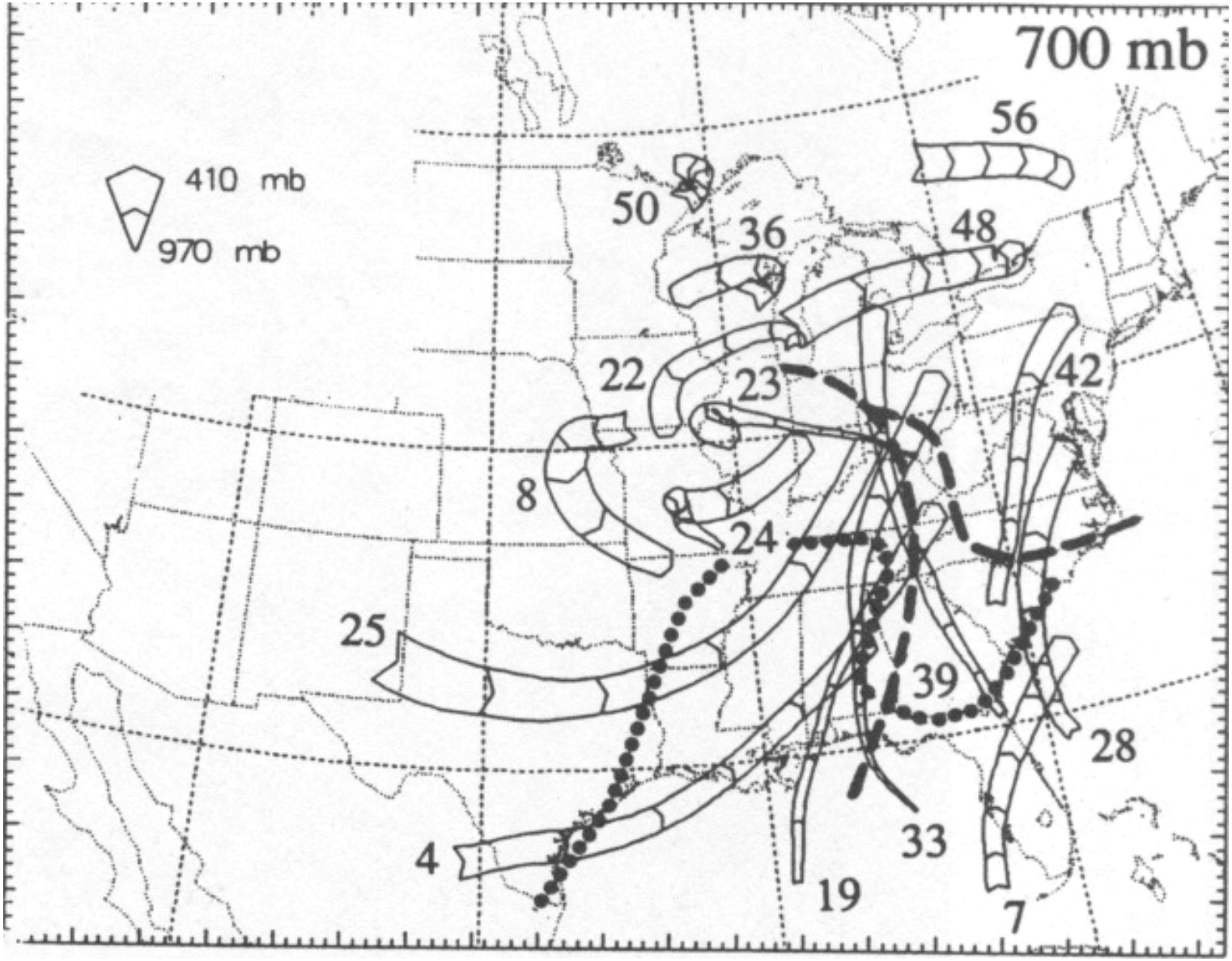
700 mb
410 mb
970 mb
56
50
36
48
22
23
42
8
24
25
39
28
33
4
19
7

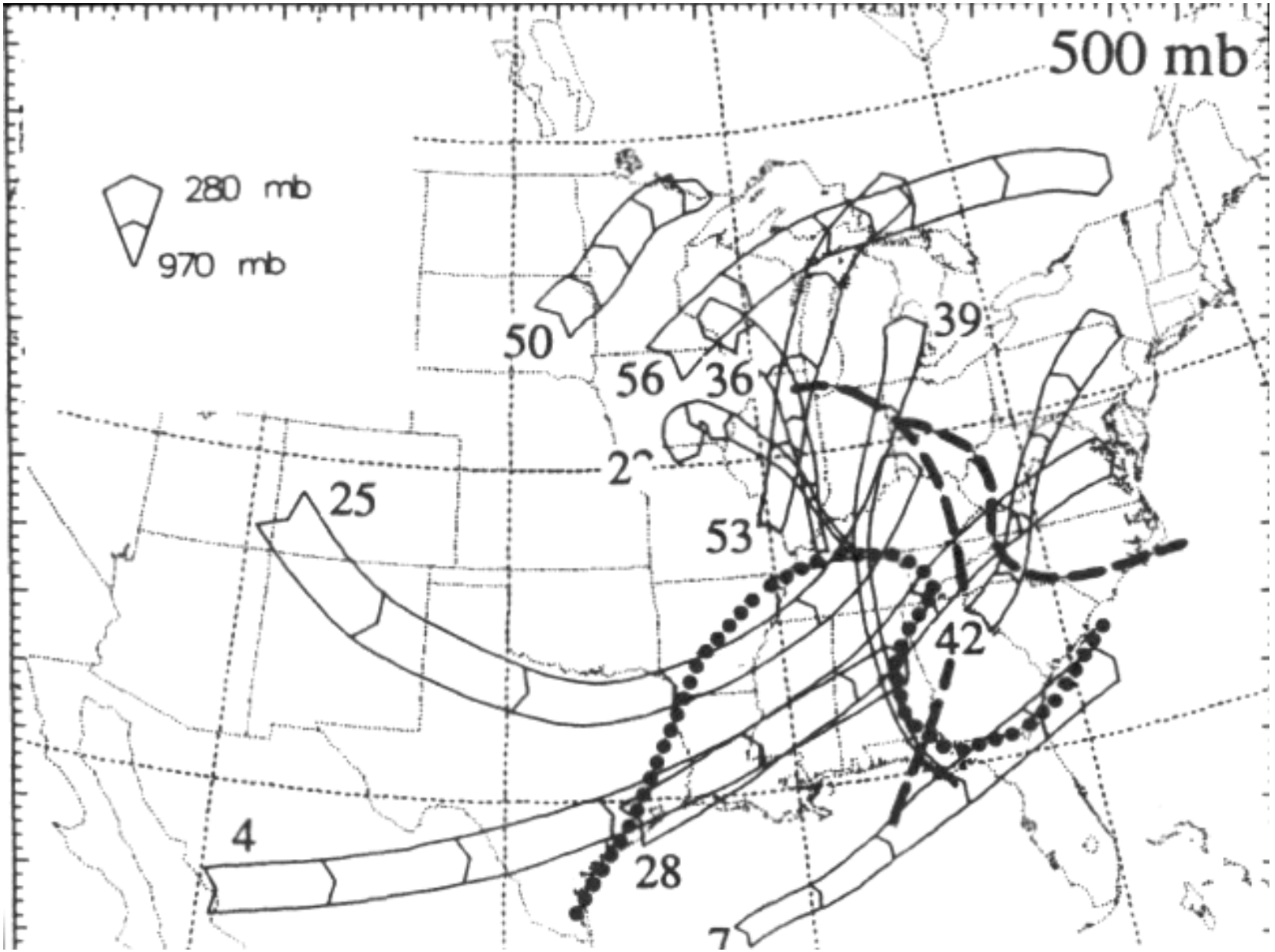
500 mb
280 mb
970 mb
50
56
36
39
25
53
42
4
28
7

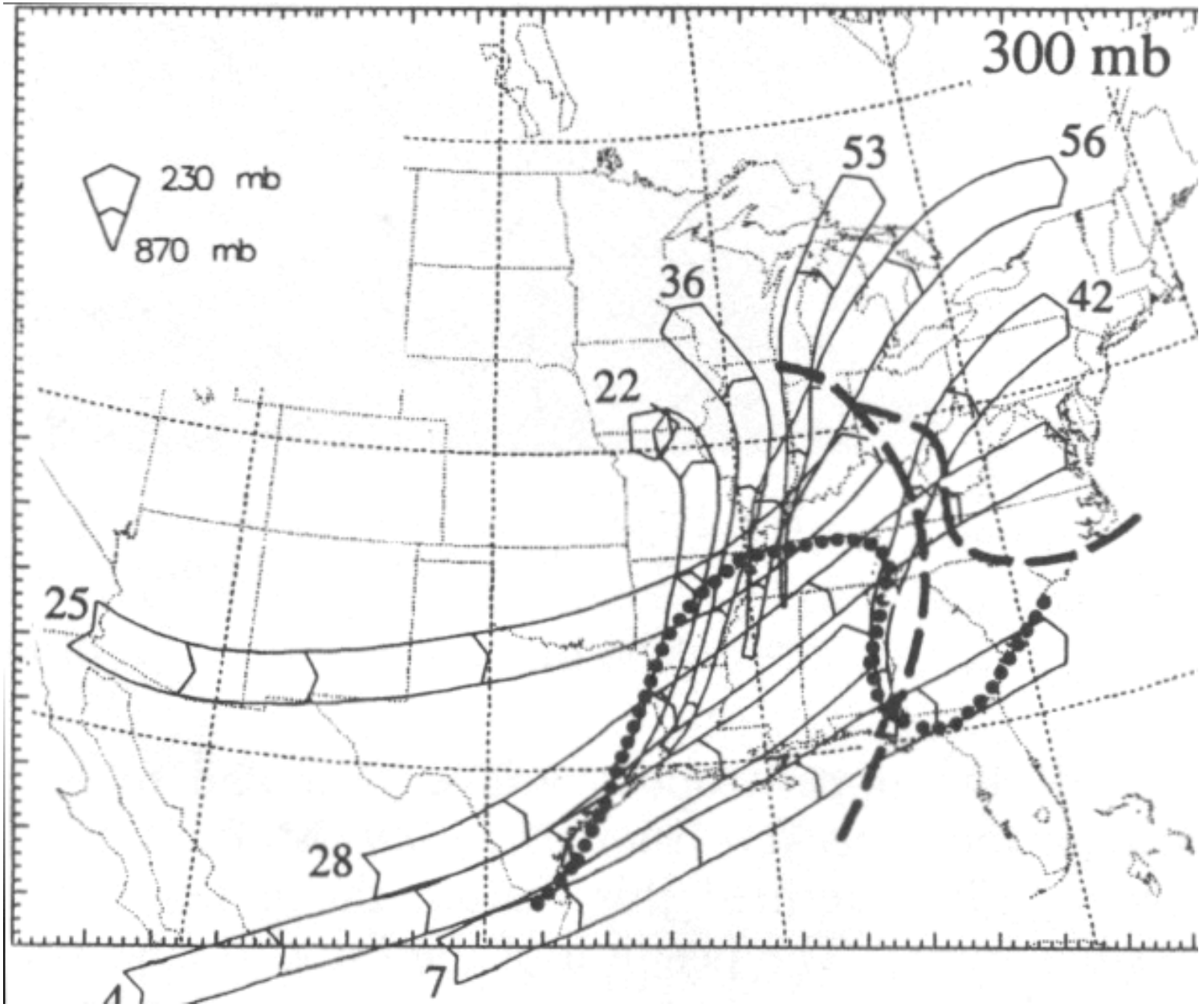
300 mb
230 mb
870 mb
53
56
36
42
22
25
28
7
4

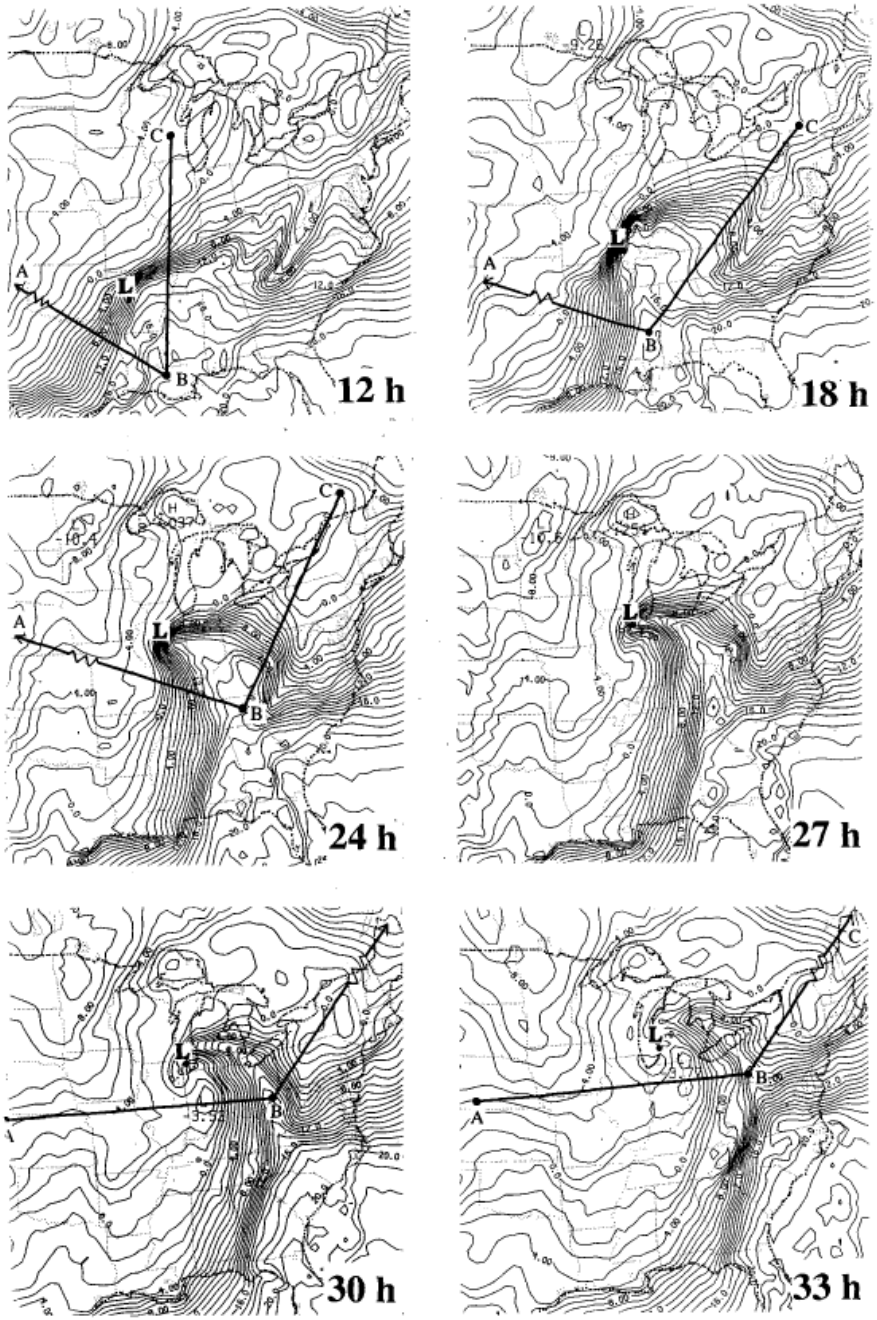

FIG. 12. Surface temperature evolution (1°C contour interval) at 12, 18, 24, 27, 30, and 33 h into the simulation (nominally 0000 UTC 15 December through 2100 UTC 15 December 1987). Model surface low positions and the locations of the vertical cross sections displayed in Schultz and Mass (1993) are also shown.

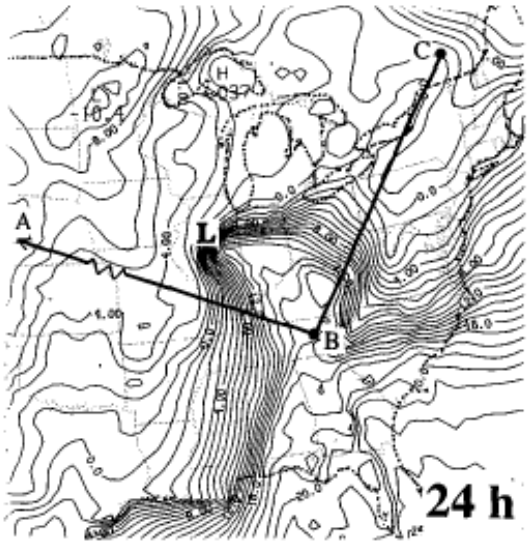
A
B
C
L
H
24 h

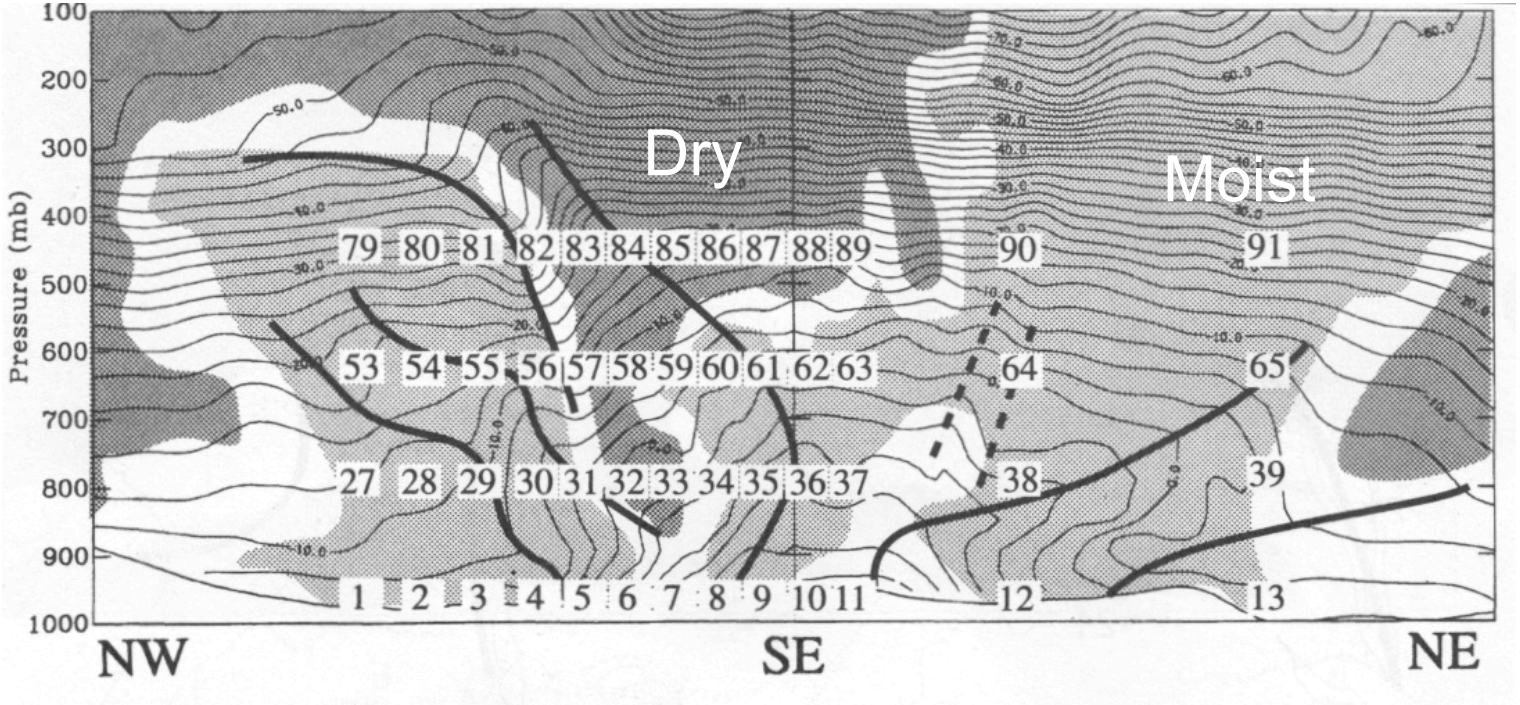
Dry
Moist
Pressure (mb)
100
200
300
400
500
600
700
800
900
1000
79 80 81 82 83 84 85 86 87 88 89 90 91
53 54 55 56 57 58 59 60 61 62 63 64 65
27 28 29 30 31 32 33 34 35 36 37 38 39
1 2 3 4 5 6 7 8 9 10 11 12 13
NW
SE
NE

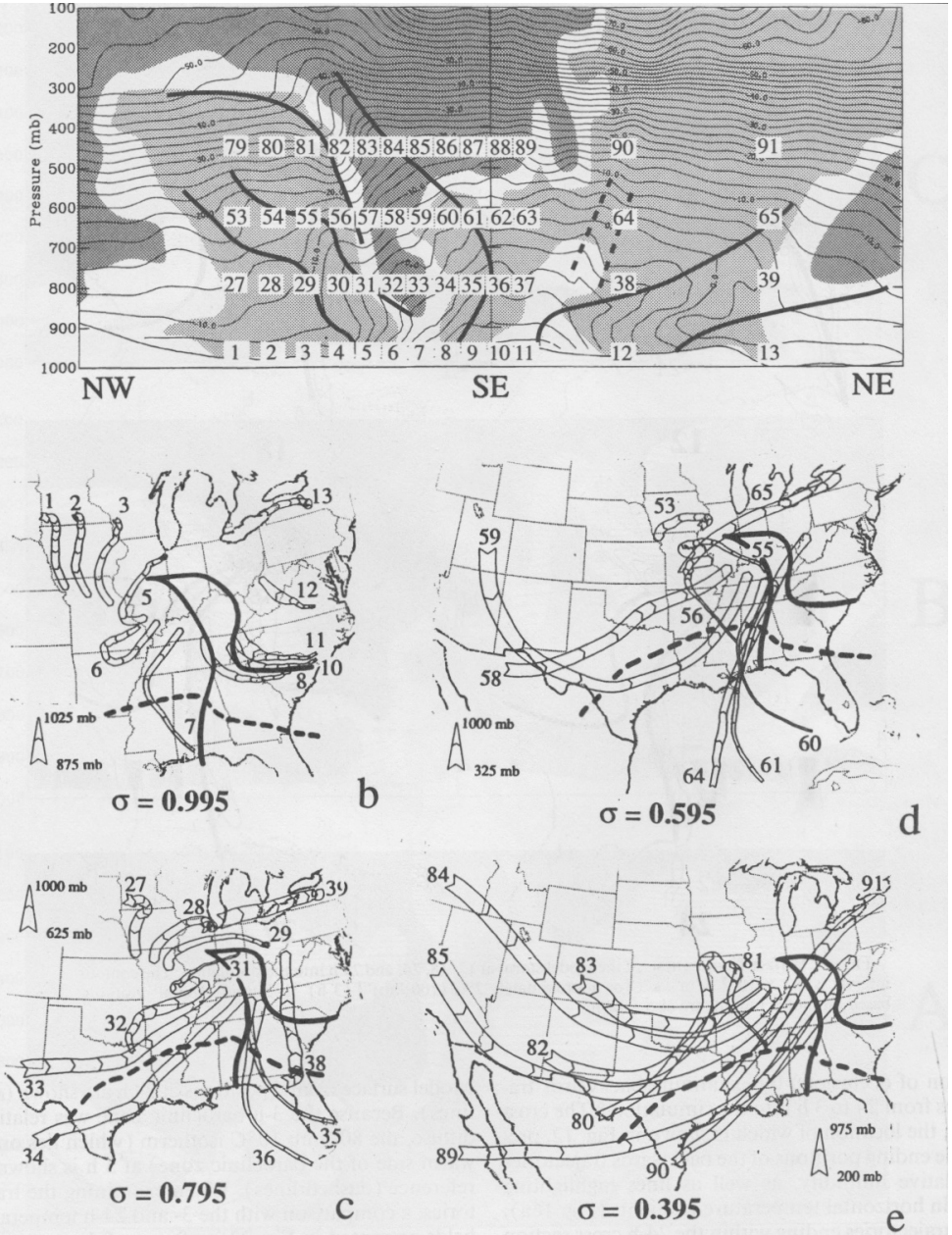

FIG. 16. (a) Vertical cross section of temperature and relative humidity at 24 h into the simulation. The temperature contour interval is 2°C and relative humidities greater than 90% and less than 40% are indicated by light and dark shading, respectively. The location of the cross section is shown in Fig. 12. Also shown are the ending positions of a number of backward trajectories (24 to 3 h). Backward trajectories from 24 to 3 h that ended in the cross section at the $\sigma = 0.995$ (b), 0.795 (c), 0.595 (d), and 0.395 (e) model levels. The 24-h model surface frontal positions (solid) and the 800-mb

Can We Use Trajectories to Understand Why Precipitation Leads the Cold Front?

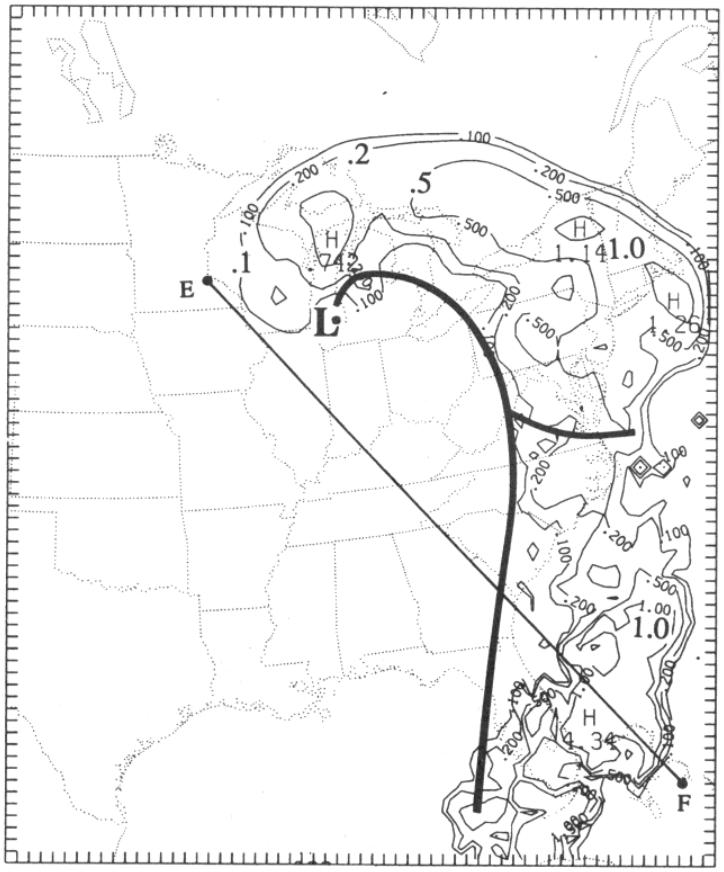

FIG. 20. Total precipitation (cm) produced by the model from 33 to 36 h into the simulation (nominally 2100 UTC 15 December through 0000 UTC 16 December 1987). The position of the cross section presented in Fig. 21 and the model fronts at 33 h are also shown.

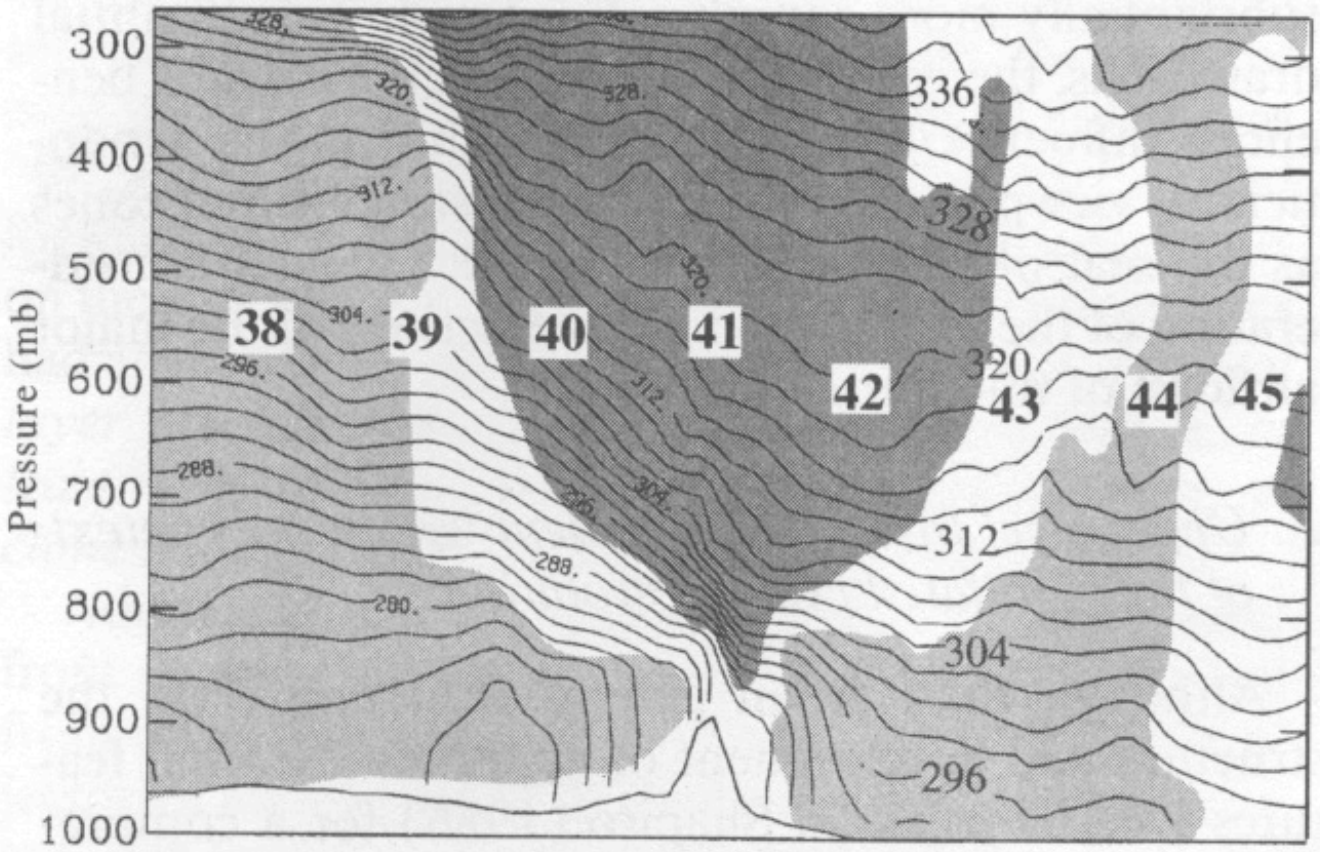

FIG. 21. Vertical cross section of potential temperature (K) and relative humidity (%) at 33 h along the path indicated in Fig. 20. The temperature interval is 2 K and relative humidities greater than 90% and less than 40% are indicated by light and dark shading, respectively. The ending points of a series of backward trajectories are also shown.

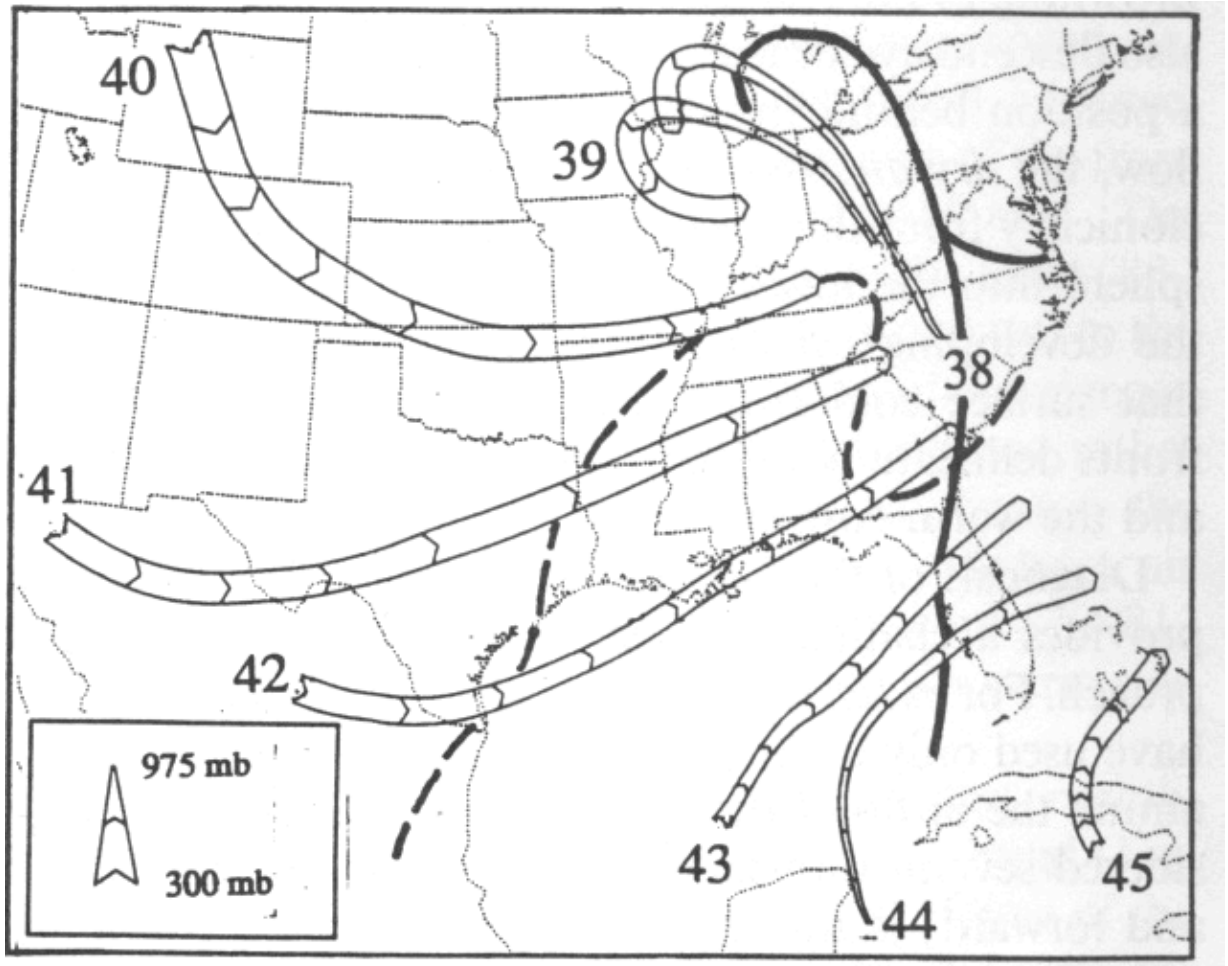

FIG. 22. Backward trajectories (from 33 to 12 h into the simulation) using model data that terminated along a line at $\sigma = 0.595$. The location of the line is shown in Figs. 20 and 21. Surface model frontal positions at 12 (dashed) and 33 h (solid) are also shown.

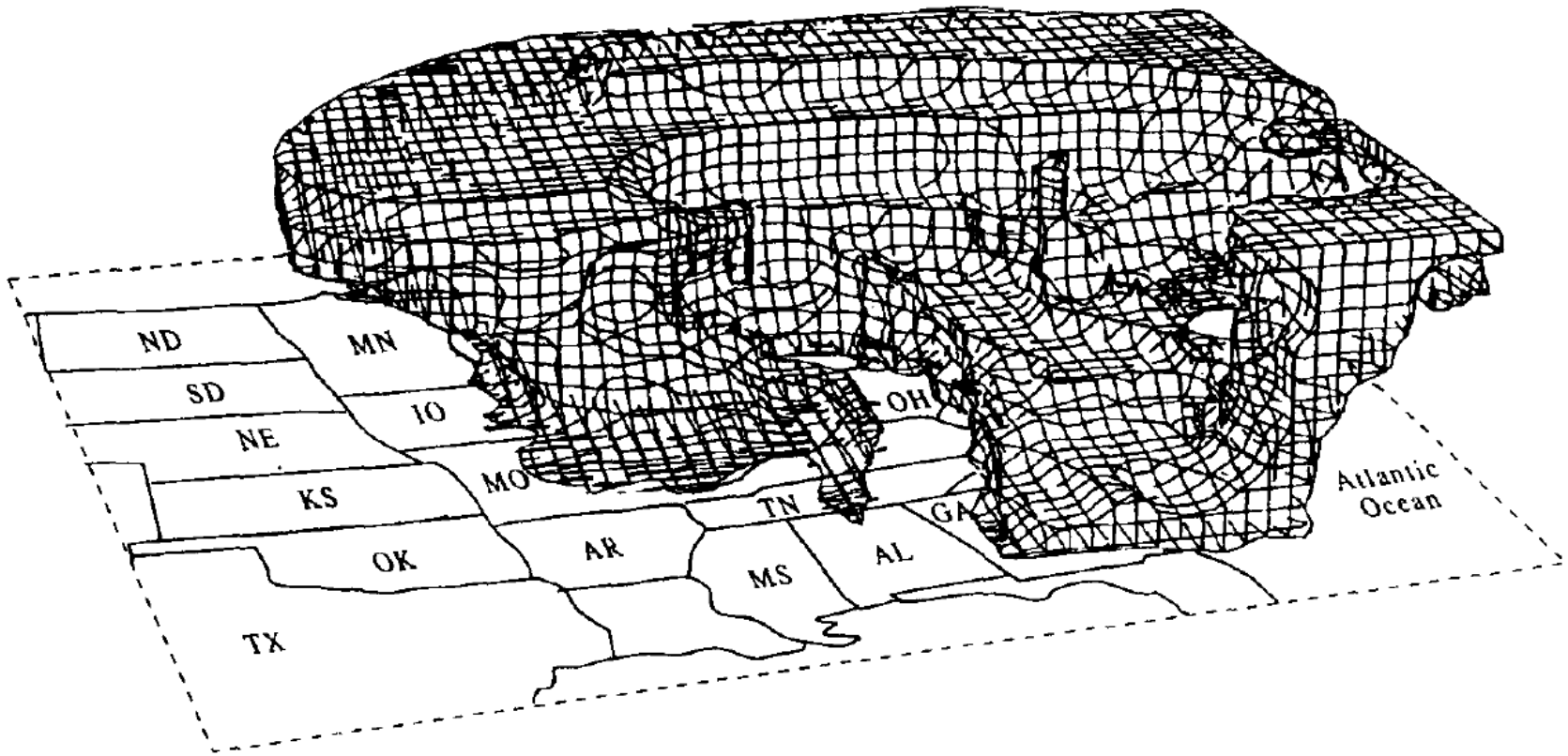

FIG. 10. Three-dimensional perspective from the south of the 100% relative humidity volume of the storm at 30 h into the simulation.

The Ocean Ranger Storm (1982)

Thermal Structure and Airflow in a Model Simulation of an Occluded Marine Cyclone

YING-HWA KUO

National Center for Atmospheric Research, Boulder, Colorado

RICHARD J. REED

Department of Atmospheric Sciences, University of Washington, Seattle, Washington

SIMON LOW-NAM

*National Center for Atmospheric Research, Boulder, Colorado**

(Manuscript received 7 May 1991, in final form 23 December 1991)

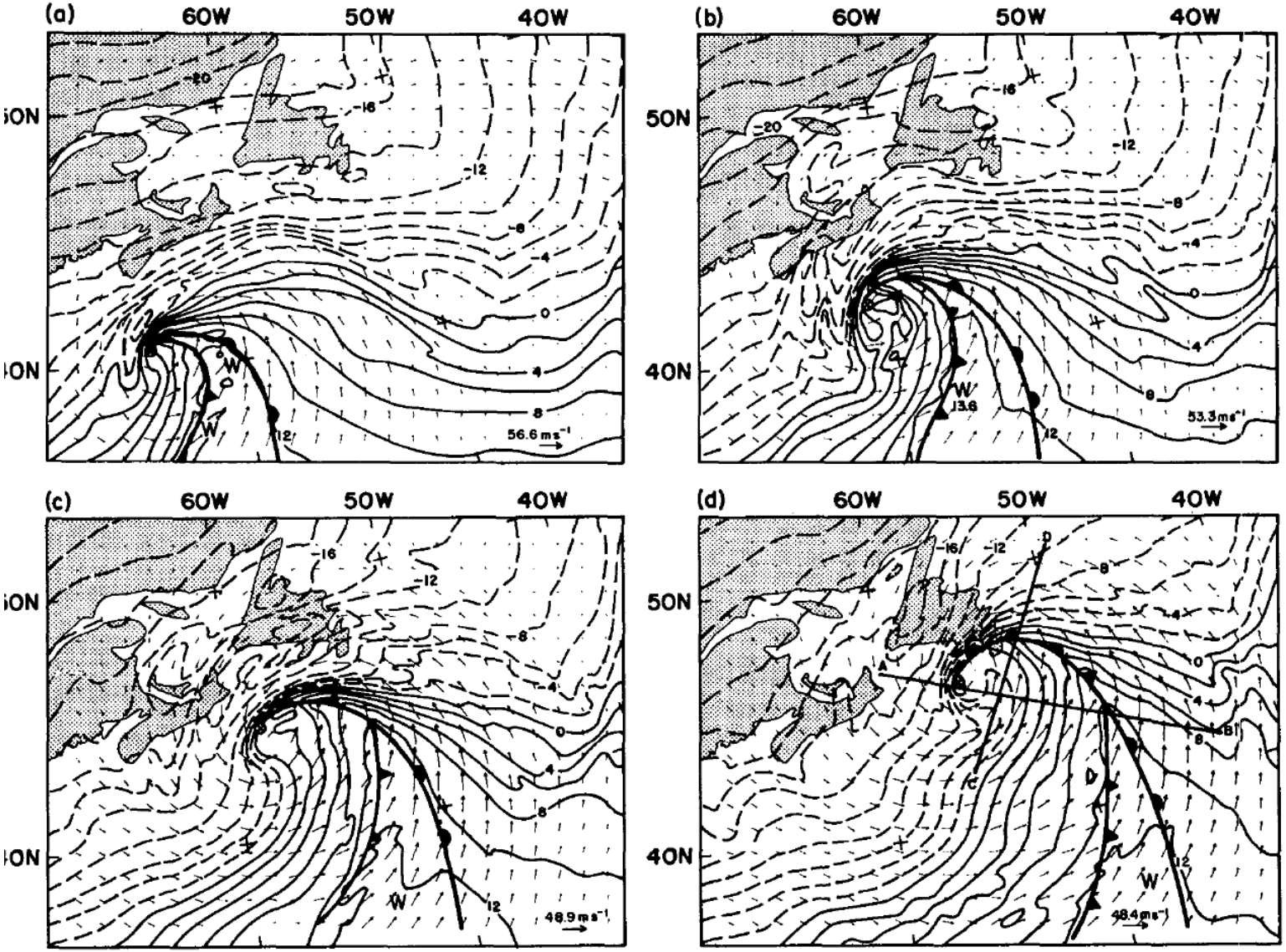

FIG. 6. The predicted 900-mb temperature (°C) and wind field valid at (a) 0000 UTC, (b) 0430 UTC, (c) 0900 UTC, and (d) 1330 UTC 14 February. Subjectively determined frontal positions are also shown.

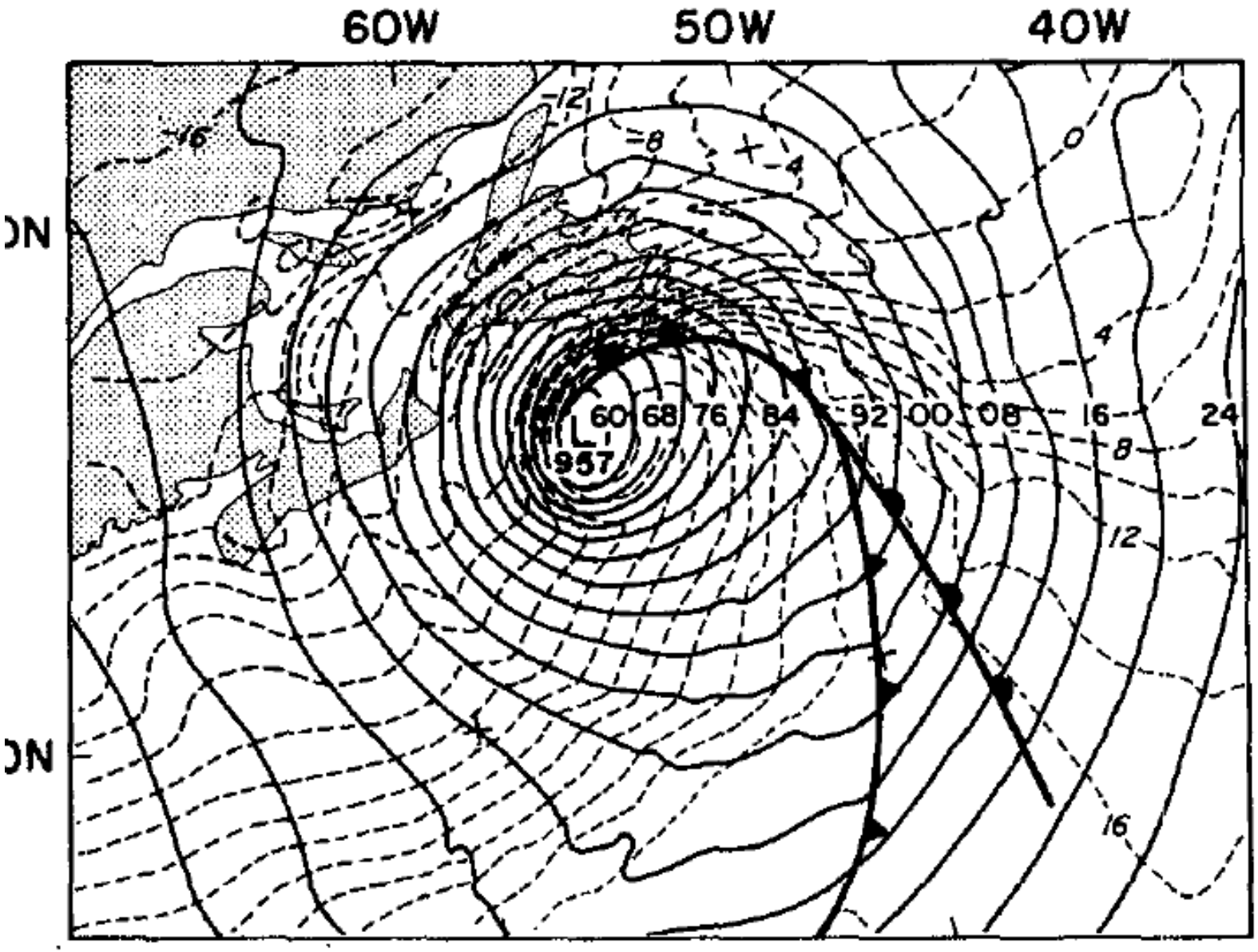

FIG. 3. The 15-h prediction of sea level pressure (solid) and temperature (dashed), valid at 1200 UTC 14 February 1982.

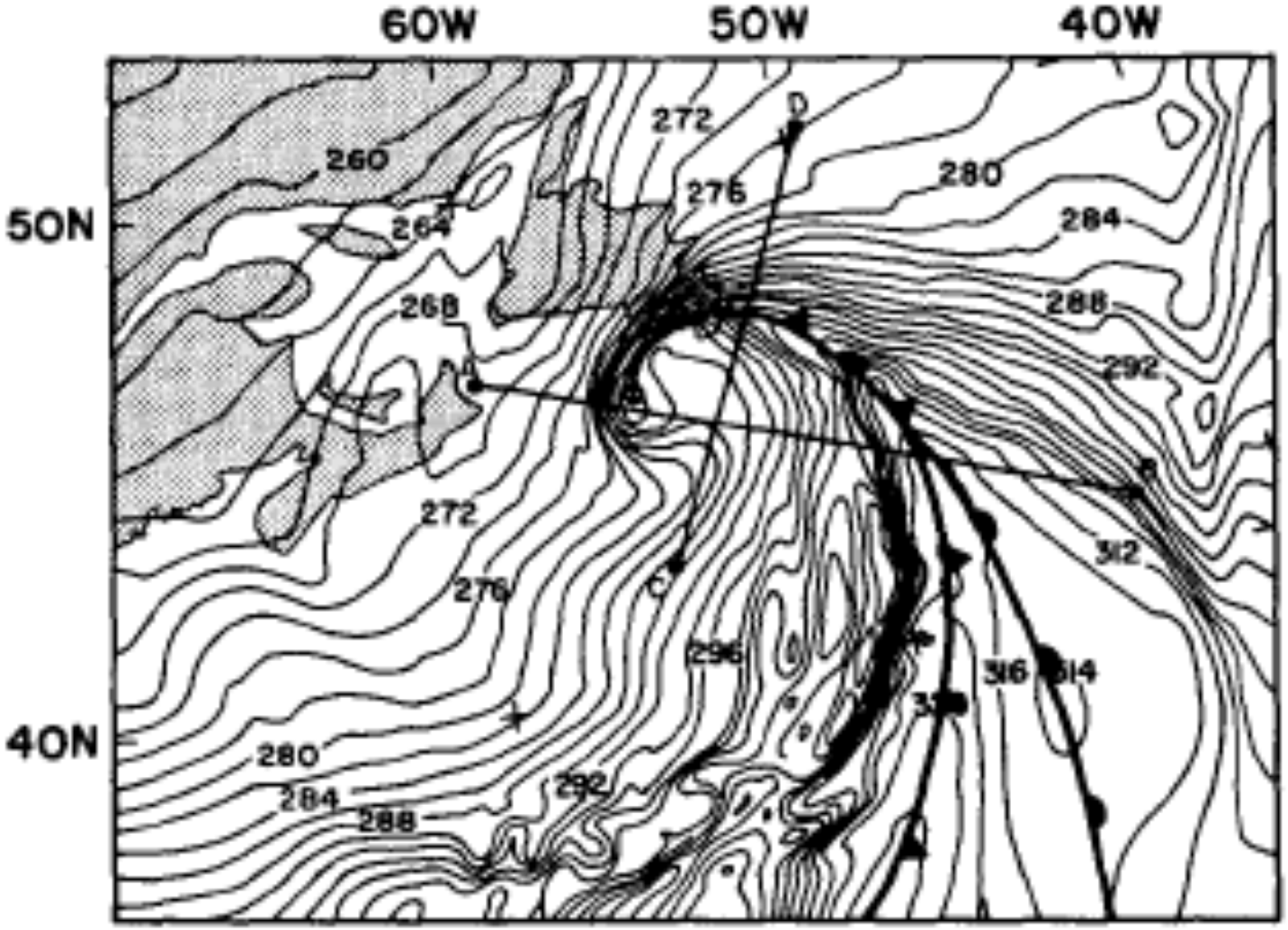

FIG. 7. The predicted 900-mb equivalent potential temperature (K) valid at 1330 UTC 14 February 1982.

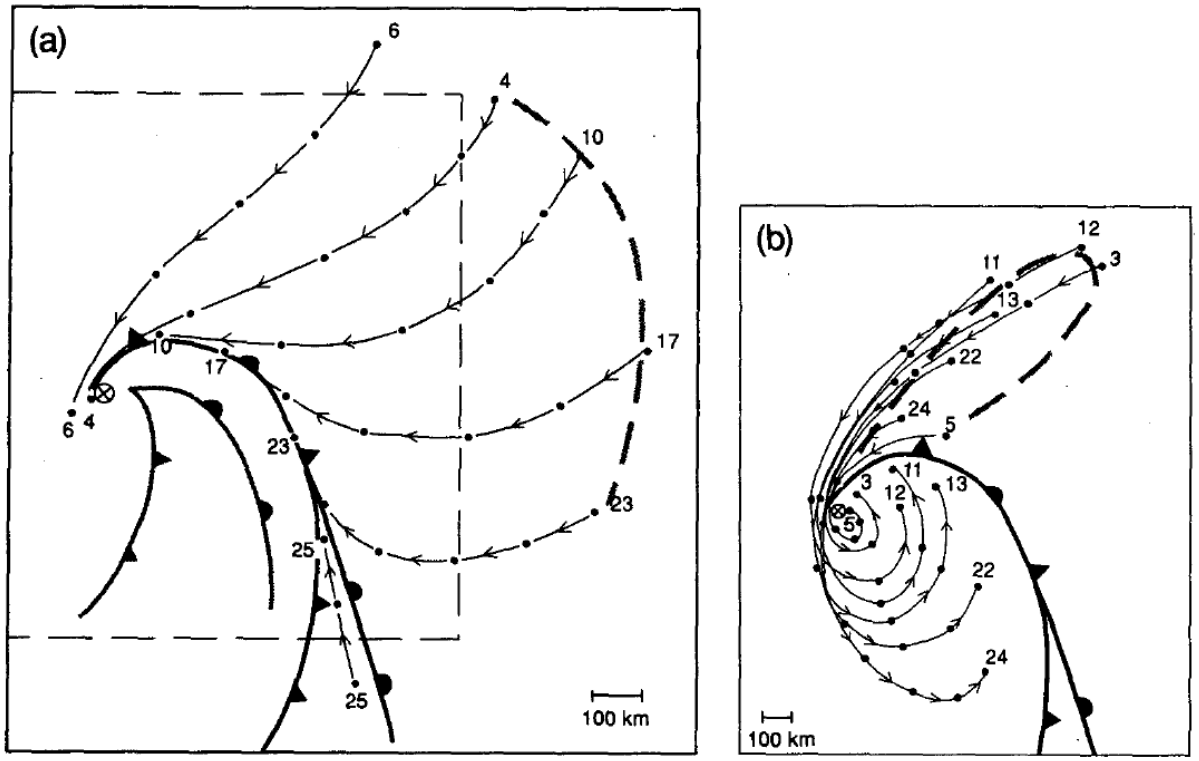

FIG. 8. The $\sigma = 0.91$ (~900 mb) backward trajectories for the period from 2200 UTC 13 February to 1330 UTC 14 February, for (a) parcels to the east of the storm and far removed from it and (b) parcels closer to the surface low. Subjectively determined fronts for the beginning and ending hours are shown in (a) and for the ending time only in (b). The inset in (a) indicates the location of (b). Line segments denote air that later formed forward (a) and rear (b) sides of the occluded front.

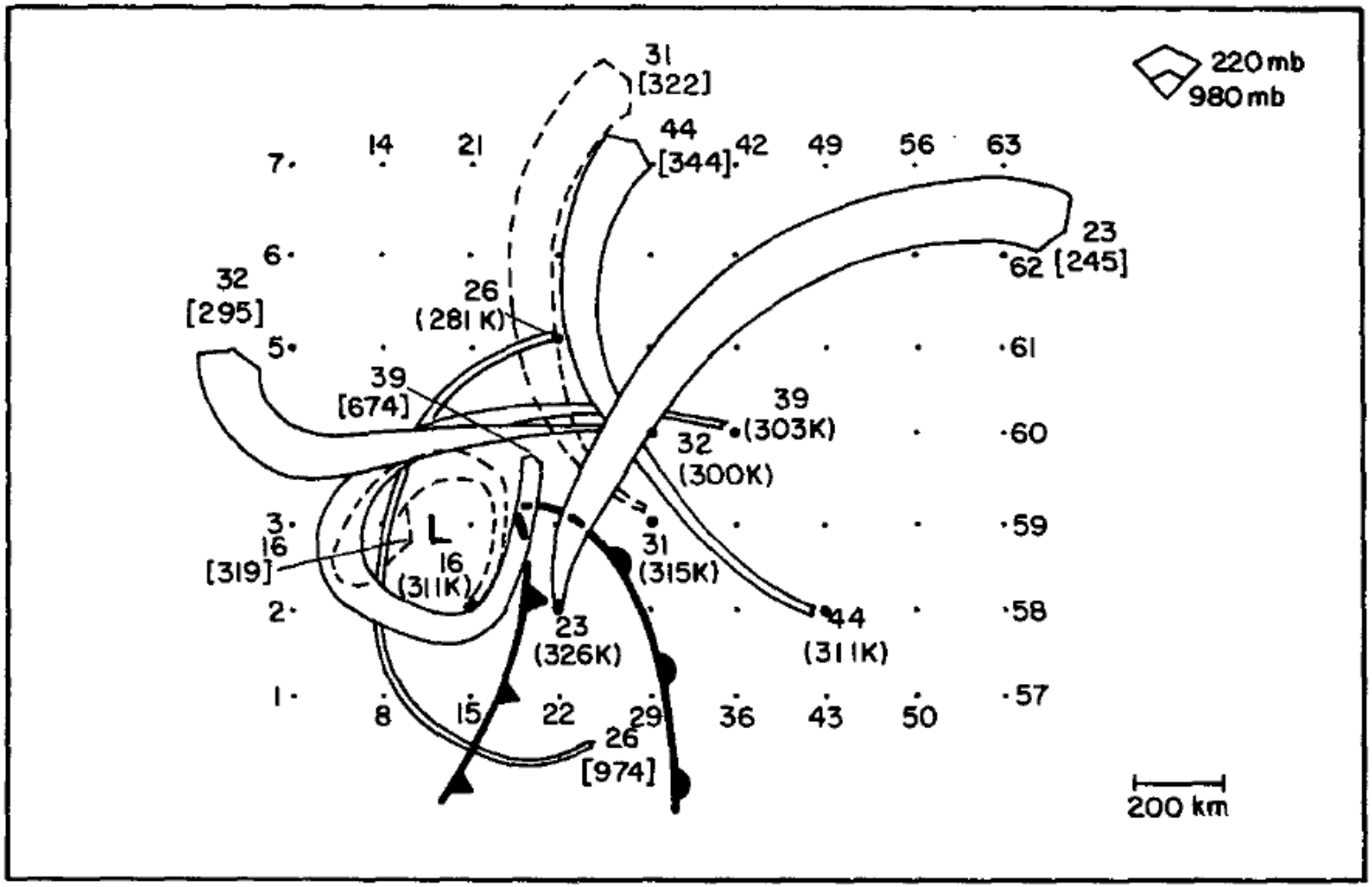

FIG. 9. The $\sigma = 0.91$ ($\sim$900 mb) forward trajectories during the period from 2200 UTC 13 February to 1330 UTC 14 February. The equivalent potential temperatures at the initial positions of the trajectories are indicated in parentheses and the ending pressures in brackets. Width of trajectories indicates pressure level according to attached scale. Initial frontal positions are also shown. For clarity, two of the trajectories are represented by dashed lines. Dots indicate starting positions of all trajectories constructed.

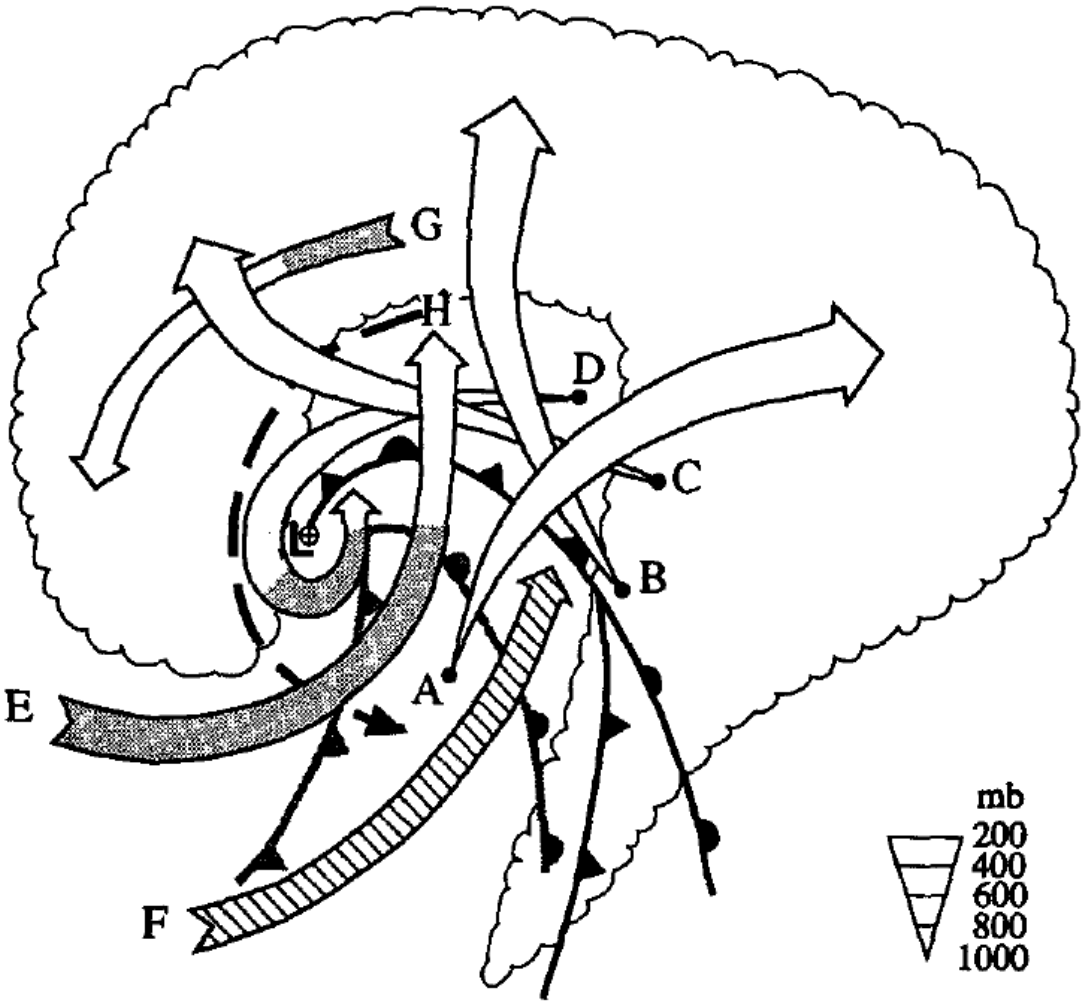

FIG. 16. Schematic diagram of the airflow in the *Ocean Ranger* storm. Fronts in open wave and occluded stages, usual convention; cloud boundary at mid- to upper levels, scalloped line; relative trajectories, arrows (open where rising, shaded where sinking, hatched where level); scale for pressure level, lower right.